7-9.1 Potter Horn

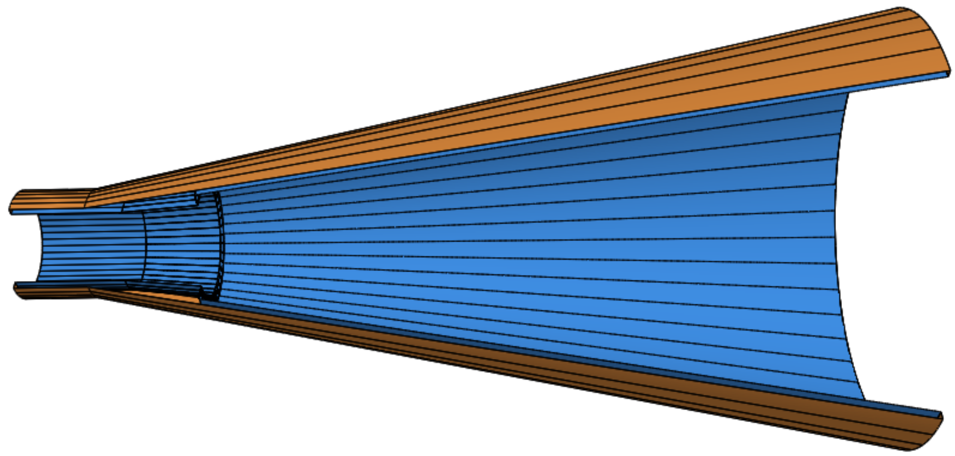

Figure 7-9.1-1 3-d Diagram of 20 dB Potter Horn

Figure 7-9.1-1 shows the design for a dual mode circular waveguide horn to generate the hybrid mode [37a]. An initial waveguide step at the input generates the TM_{11} mode at the correct level for a hybrid mode. This horn was design empirically over the range from 13- to 24-dB and a series of design curves was produced [37a]. These designs start with an input waveguide radius, $a_i = 0.51\lambda_c$ and a step radius, $a_s = 0.65\lambda_c$.

Starting with these dimensions, an optimization within a mode-matching analysis, examples: CHAMP (TICRA) or Mician *MicroWave Wizard*, quickly produces a design with desired parameters. However, the design equations will produce a design very close to the desired gain that radiates in the hybrid mode with low cross polarization in the diagonal plane. A horn designed for 20 dB gain had an 8% 25 dB cross polarization bandwidth and 14% at 20 dB. Horns design with lower gains had similar bandwidths to the 20 dB case.

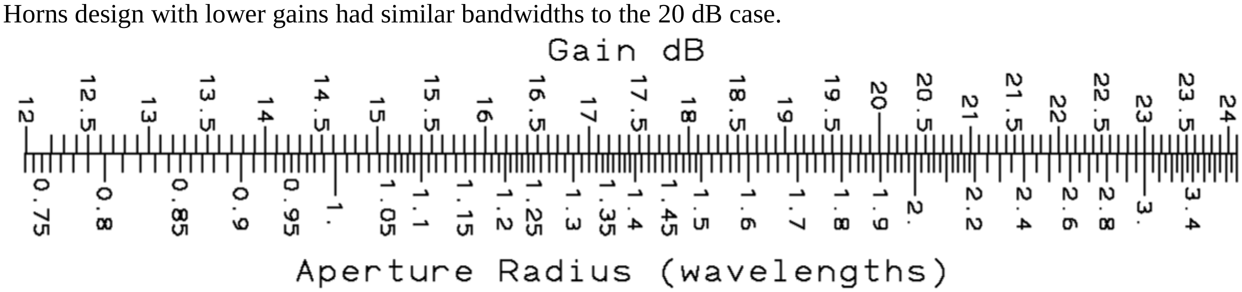

Potter Horn Aperture Radius versus Gain

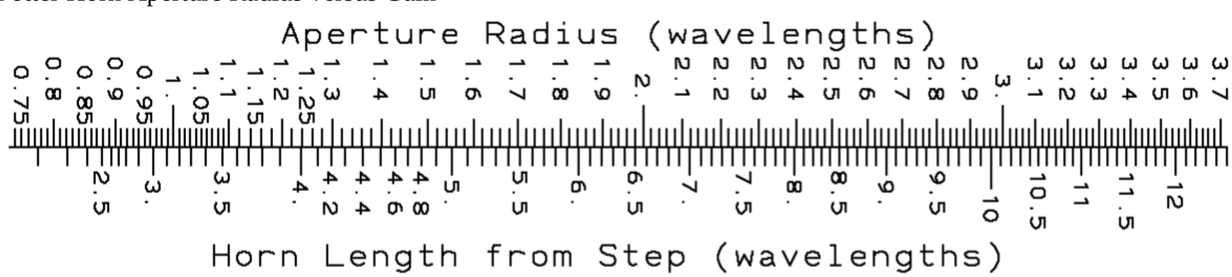

Potter Horn Axial Length from Step given Aperture Radius

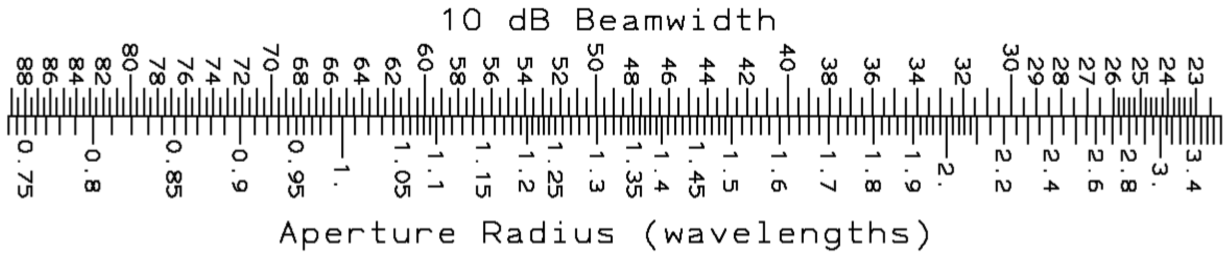

Potter Horn 10 dB Beamwidth versus Aperture Radius

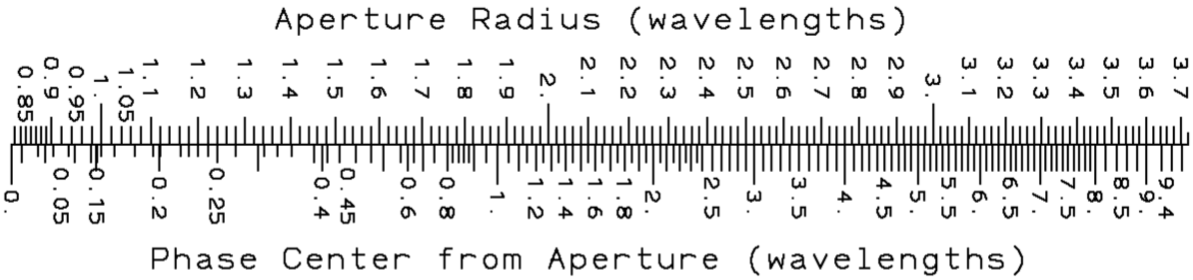

Potter Horn Average Phase Center given Aperture Radius

Table 7-9.1 Potter Horn Design Parameters

Gain dB	Aperture Radius, λ	Axial Length from Step, λ	25-dB Max X-pol. BW %	10-dB Beamwidth	Phase Center, λ
13.0	0.8254	2.3116	9.3	79.2	0.002
13.5	0.8747	2.4851	6.7	74.8	0.035
14.0	0.9202	2.8087	7.8	70.2	0.050
14.5	0.9878	3.0975	7.5	66.2	0.106
15.0	1.0382	3.3268	8.0	62.1	0.168
15.5	1.1146	3.5985	7.5	58.6	0.188
16.0	1.1715	3.8301	8.2	55.1	0.243
16.5	1.2548	4.0498	7.1	52.1	0.252
17.0	1.3195	4.2795	8.8	49.0	0.292
17.5	1.4059	4.5181	7.3	46.2	0.326
18.0	1.4783	4.7799	8.4	43.5	0.415
18.5	1.5765	5.0684	7.8	41.0	0.477
19.0	1.6755	5.3927	8.2	38.6	0.634
19.5	1.7782	5.7645	8.0	36.4	0.831
20.0	1.8958	6.1891	8.6	34.3	1.033
20.5	2.0300	6.6771	8.0	32.3	1.362
21.0	2.1834	7.2330	8.0	30.5	1.781
21.5	2.3616	7.8676	8.7	28.7	2.309
22.0	2.5428	8.5903	8.0	27.1	3.094
22.5	2.7715	9.4018	7.9	25.6	4.040
23.0	2.9989	10.118	8.3	24.3	5.237
23.5	3.3407	11.341	8.2	23.2	7.272
24.0	3.7211	12.501	8.0	22.3	9.840

13.0 dB Gain Potter Horn Response

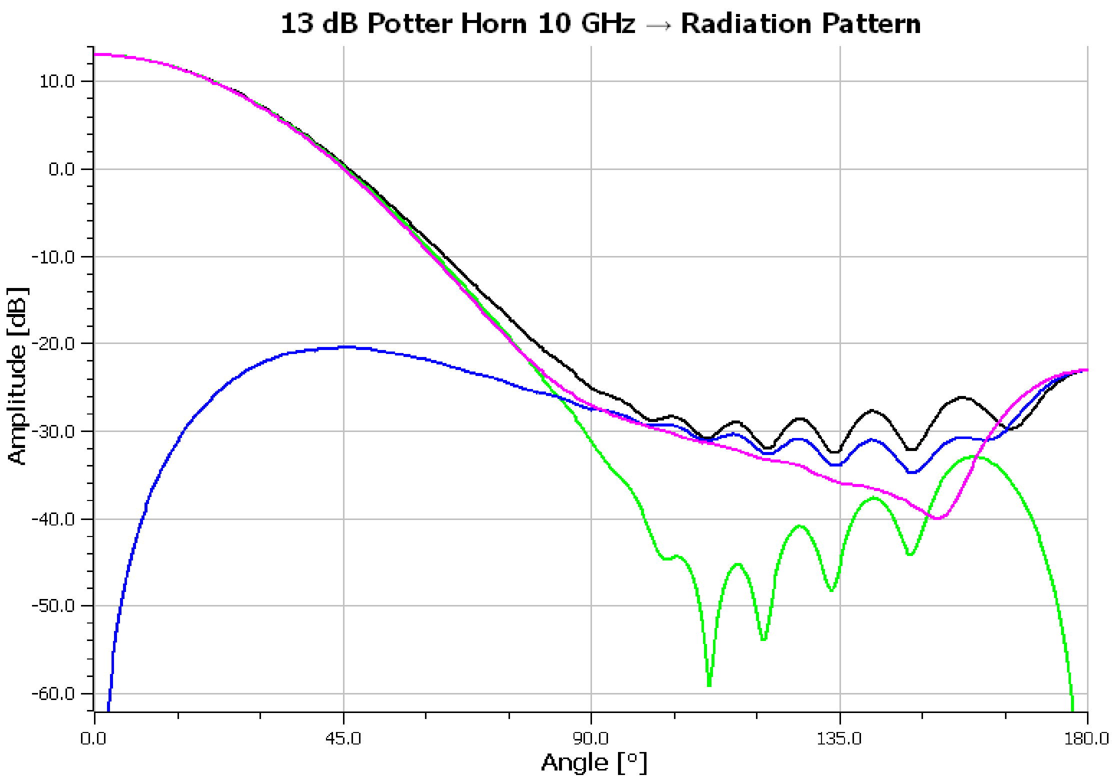

Center frequency pattern response (10 GHz)

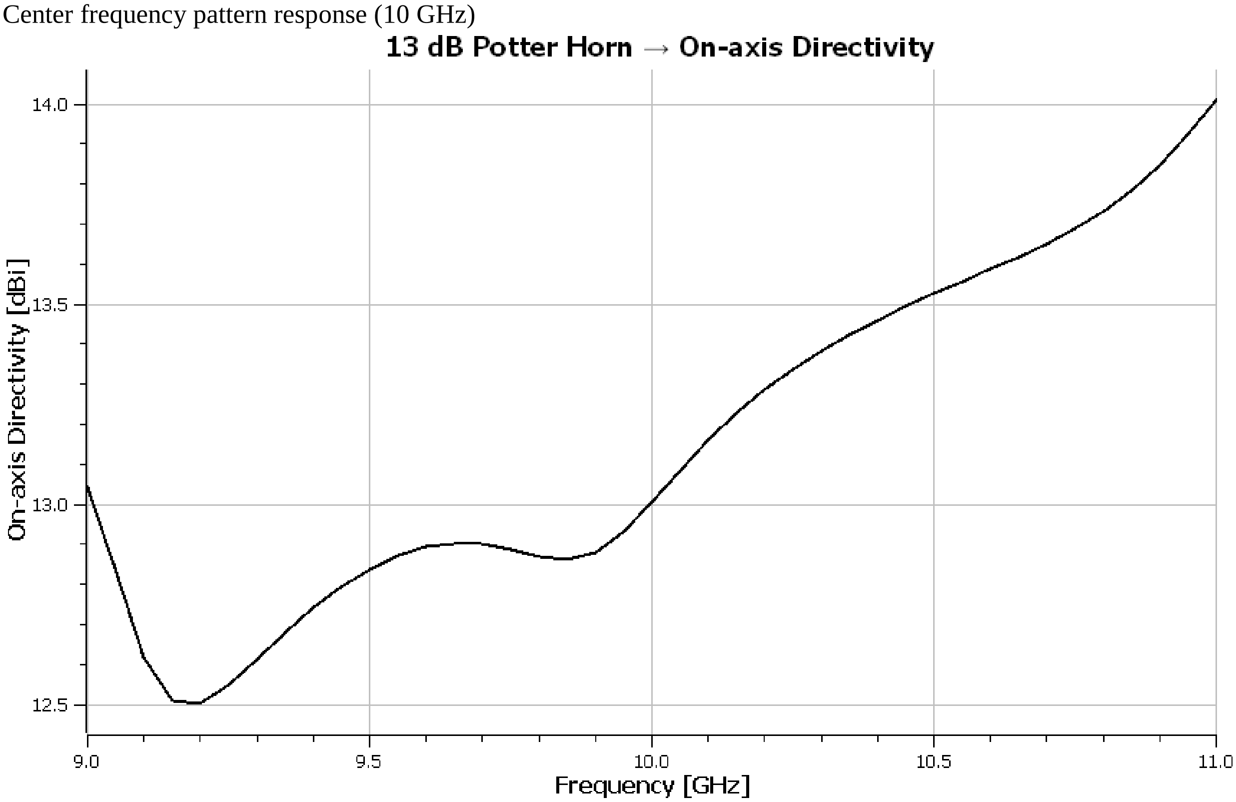

13 dB Gain Potter Horn on axis Directivity versus Frequency

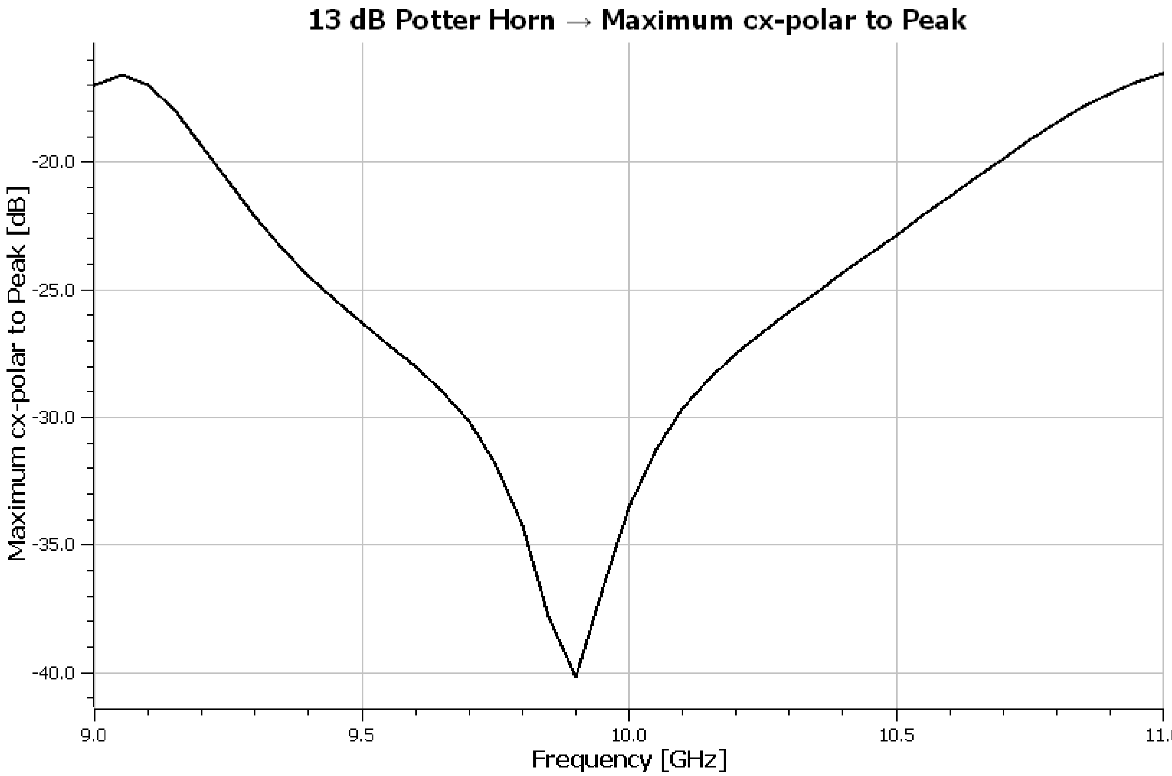

13 dB Gain Potter Horn Maximum Cross-Polarization relative to Peak versus Frequency

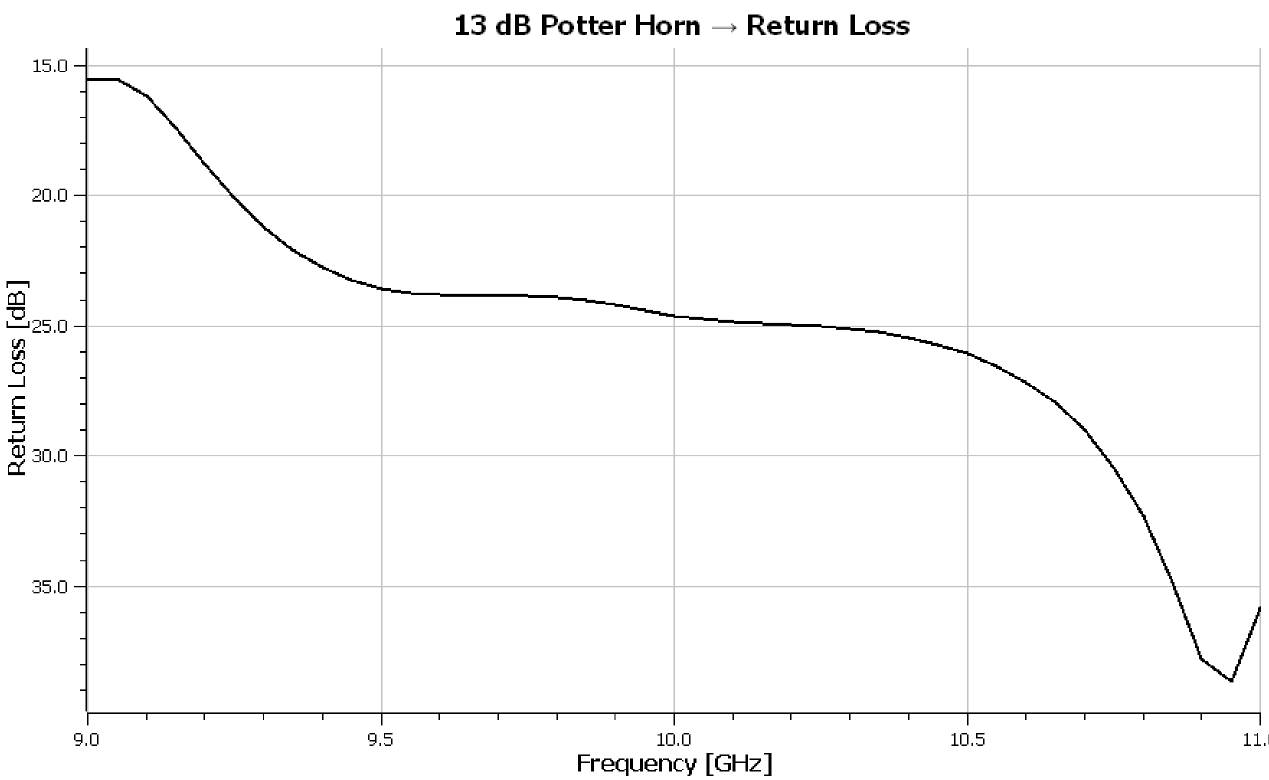

13 dB Potter Horn Return Loss relative to Peak versus Frequency

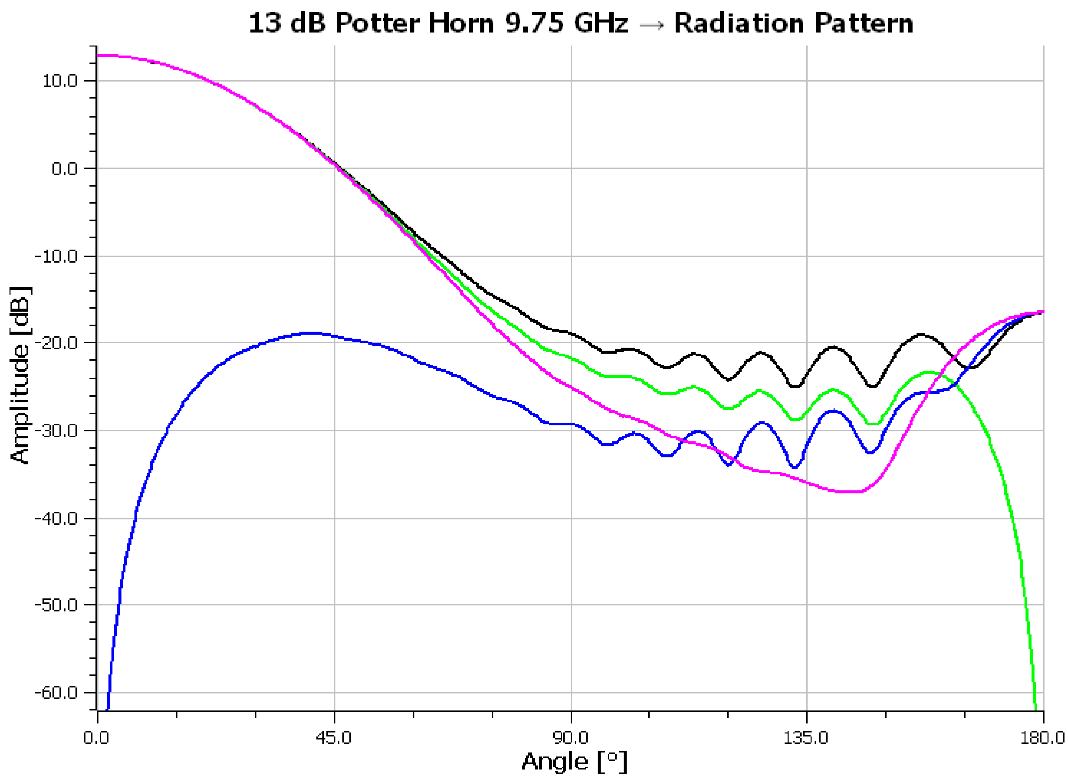
13 dB Potter Horn 9.75 GHz → Radiation Pattern
Amplitude [dB]
10.0
0.0
-10.0
-20.0
-30.0
-40.0
-50.0
-60.0
0.0
45.0
90.0
135.0
180.0
Angle [°]

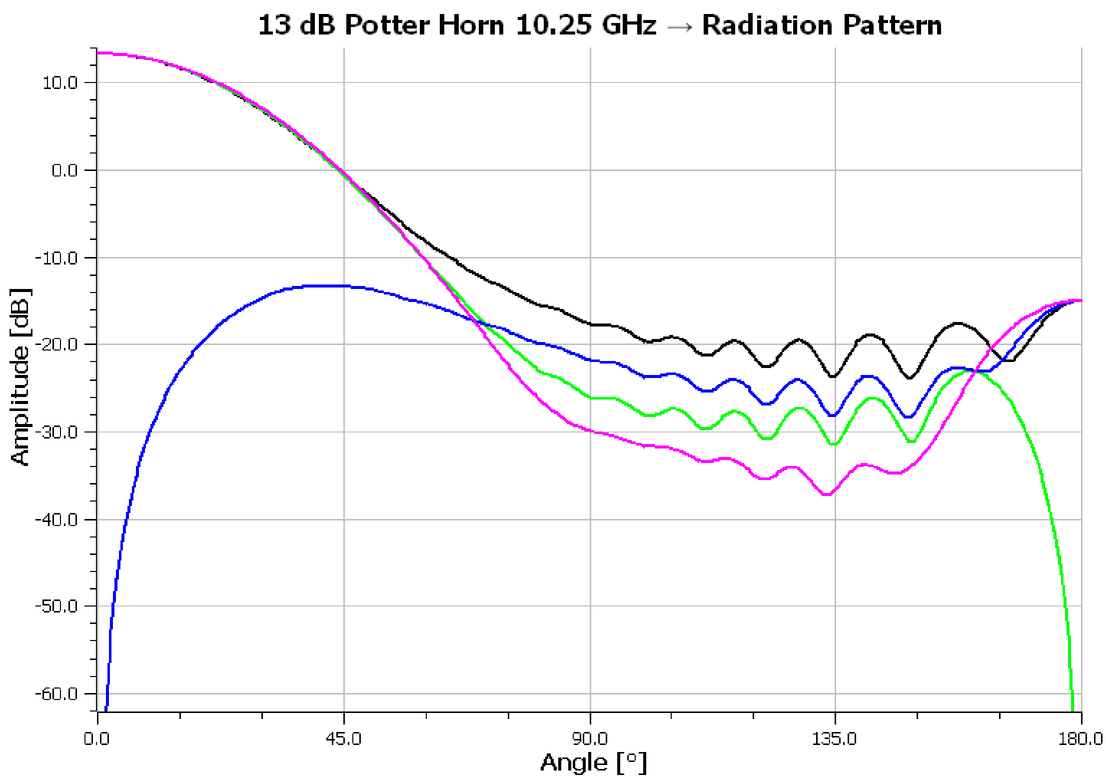
13 dB Potter Horn 10.25 GHz → Radiation Pattern
Amplitude [dB]
10.0
0.0
-10.0
-20.0
-30.0
-40.0
-50.0
-60.0
0.0
45.0
90.0
135.0
180.0
Angle [°]

18.0 dB Gain Potter Horn Response

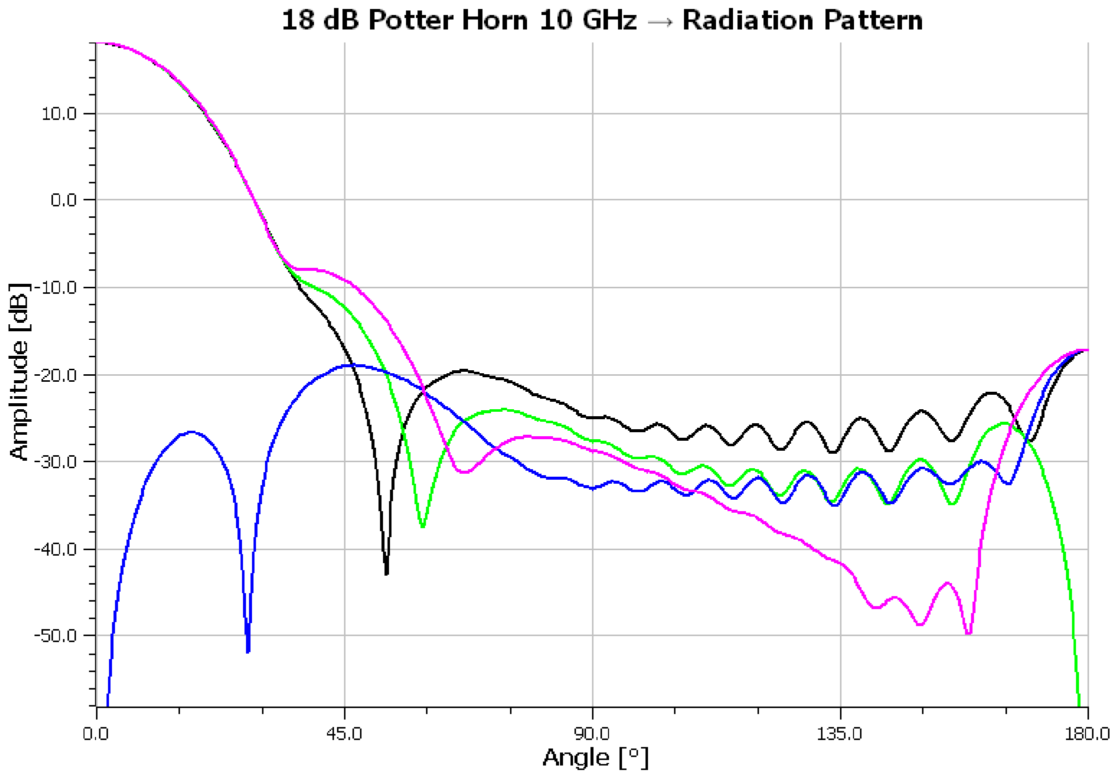

18 dB Gain Potter Horn Center Frequency Pattern (10 GHz)

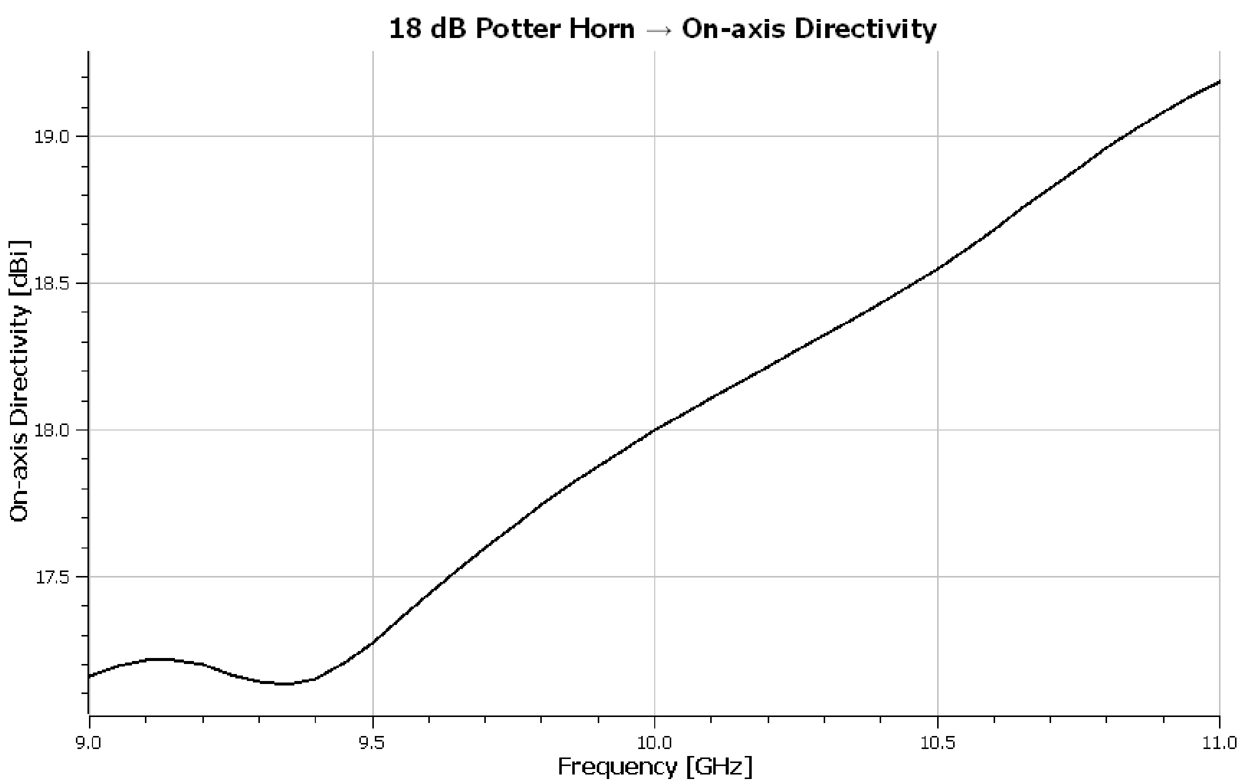

18 dB Gain Potter Horn Directivity versus Frequency

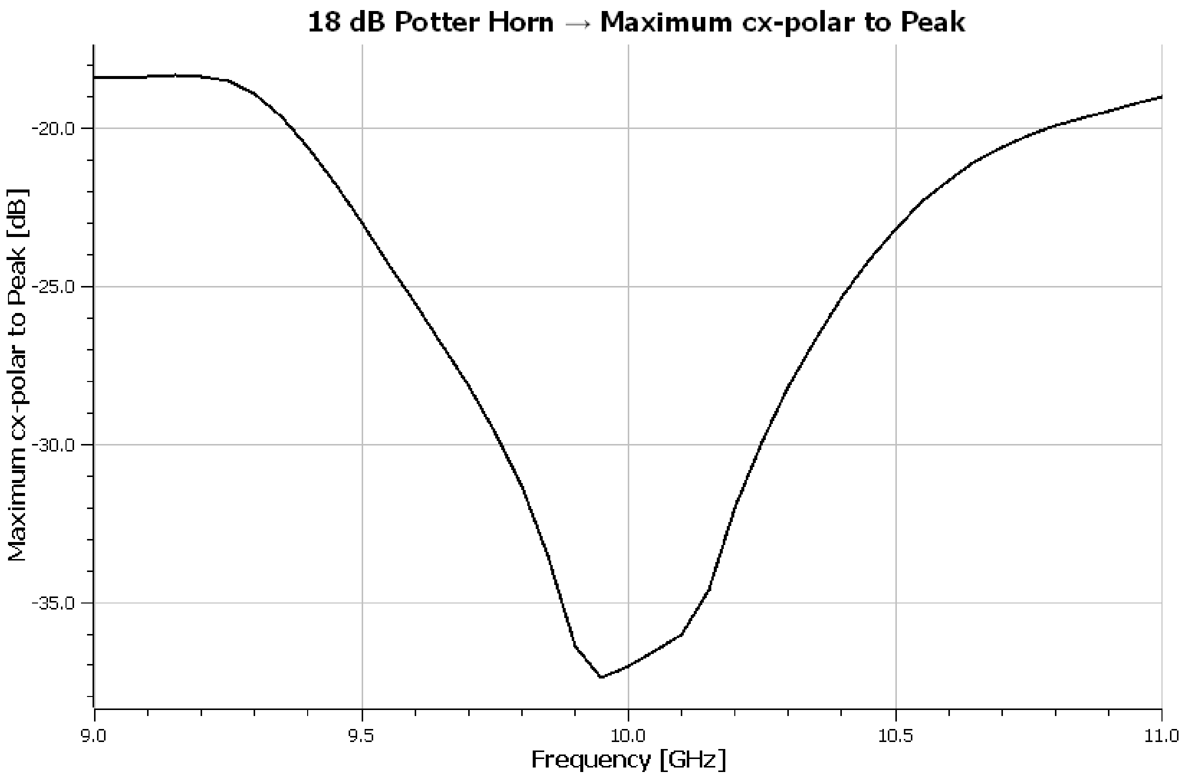

18 dB Gain Potter Horn Maximum Cross-Polarization relative to Peak versus Frequency

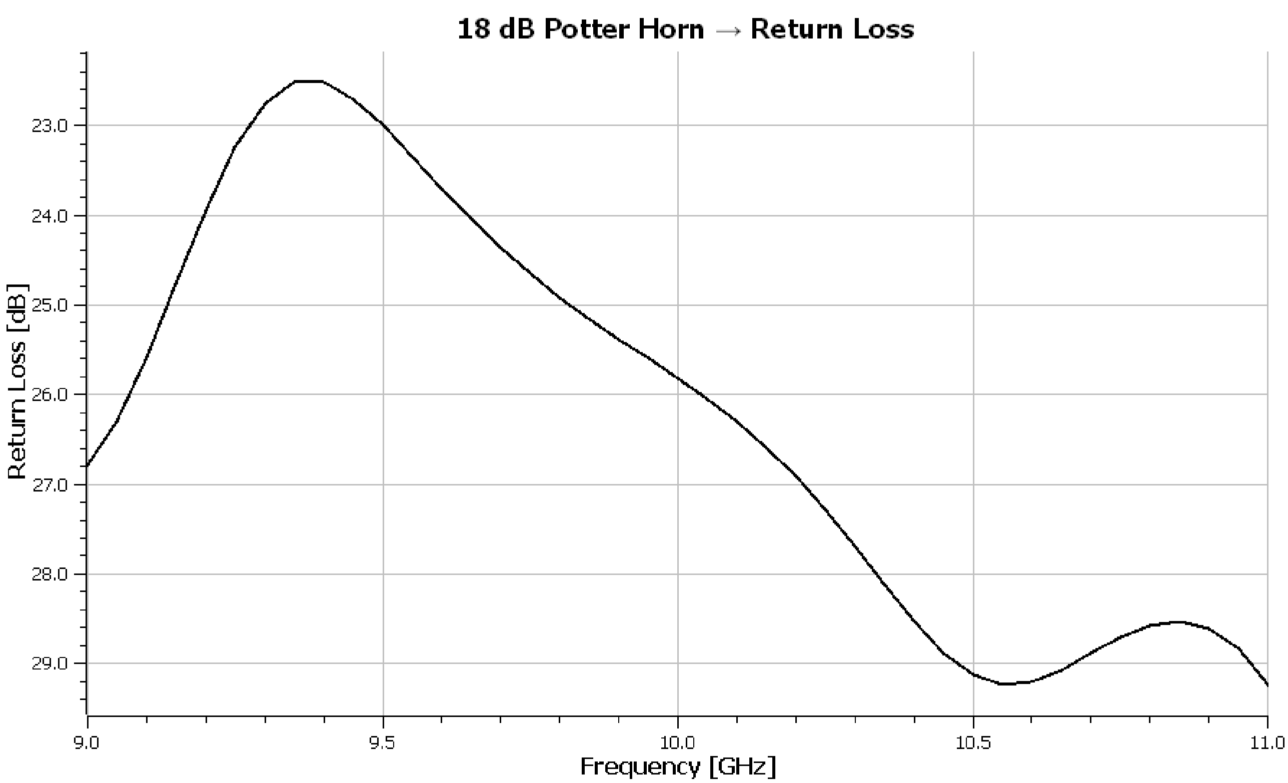

18 dB Gain Potter Horn Return Loss relative to Peak versus Frequency

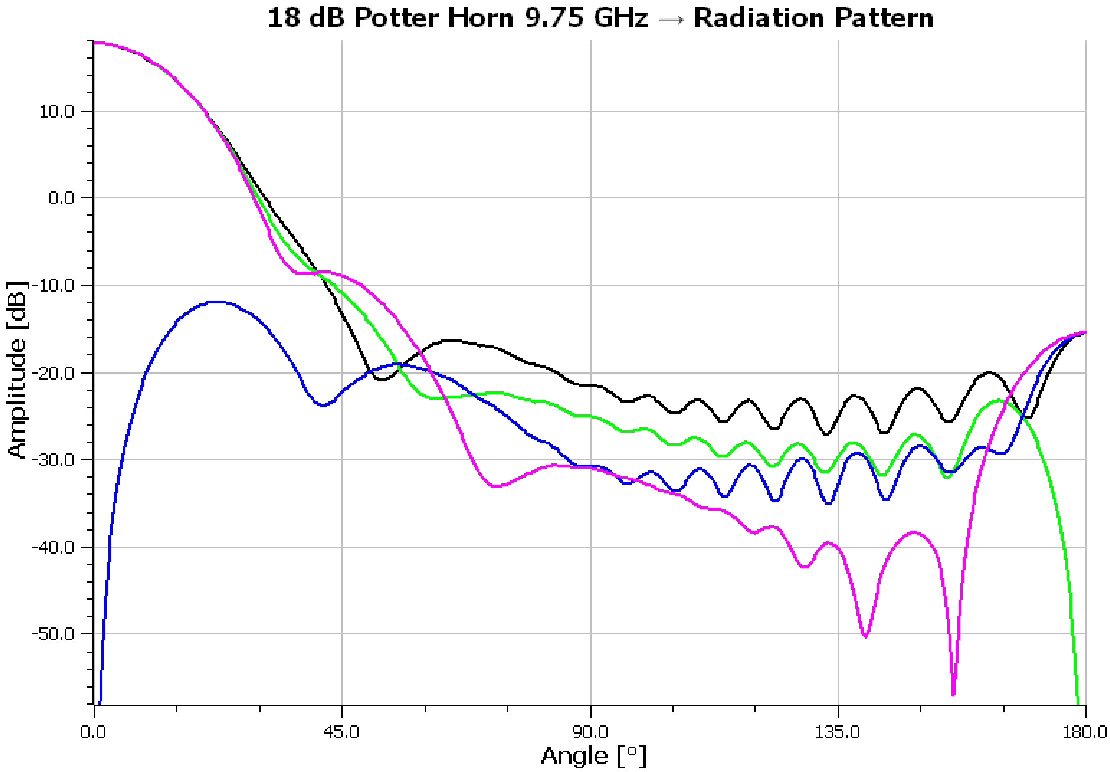
18 dB Potter Horn 9.75 GHz → Radiation Pattern
10.0
0.0
-10.0
-20.0
-30.0
-40.0
-50.0
Amplitude [dB]
0.0
45.0
90.0
135.0
180.0
Angle [°]

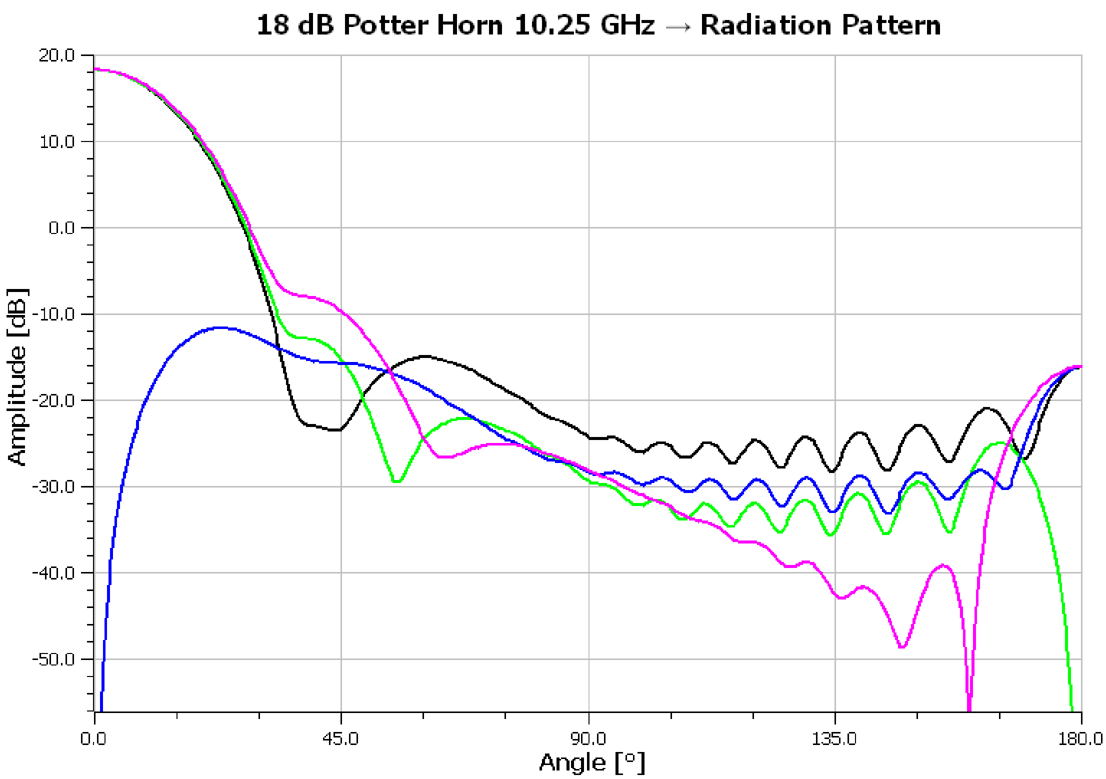
18 dB Potter Horn 10.25 GHz → Radiation Pattern
20.0
10.0
0.0
-10.0
-20.0
-30.0
-40.0
-50.0
Amplitude [dB]
0.0
45.0
90.0
135.0
180.0
Angle [°]

24.0 dB Gain Potter Horn Response

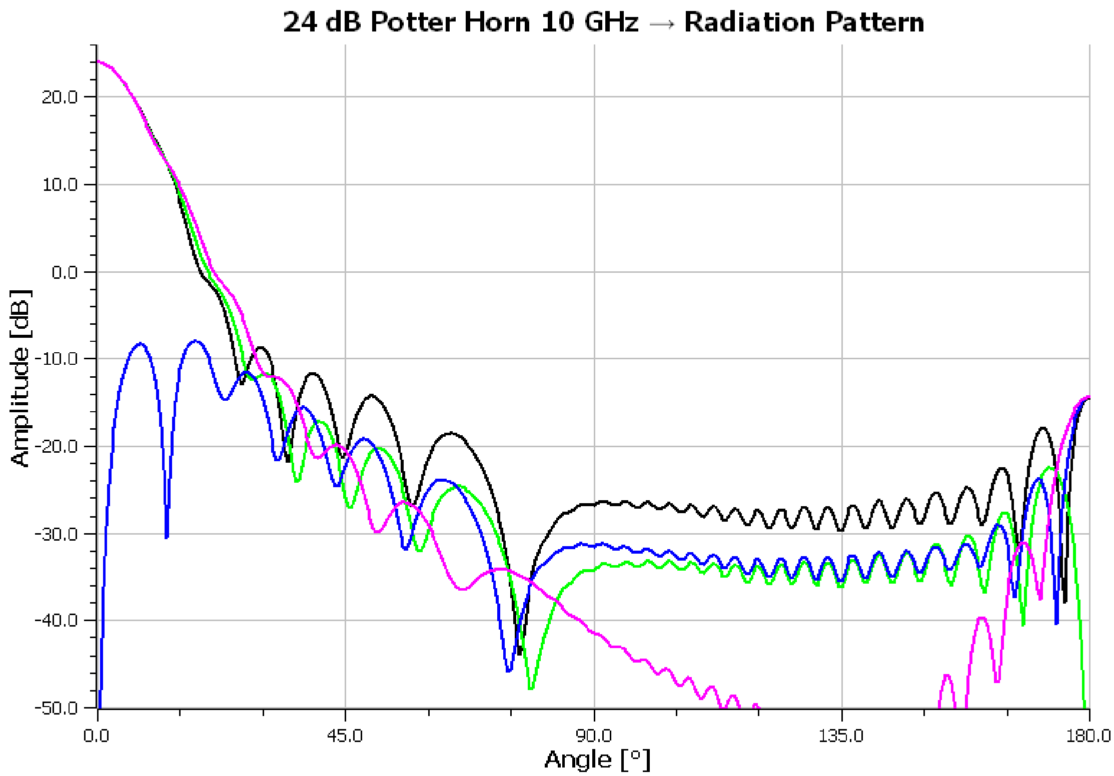

24 dB Gain Potter Horn Center Frequency Pattern (10 GHz)

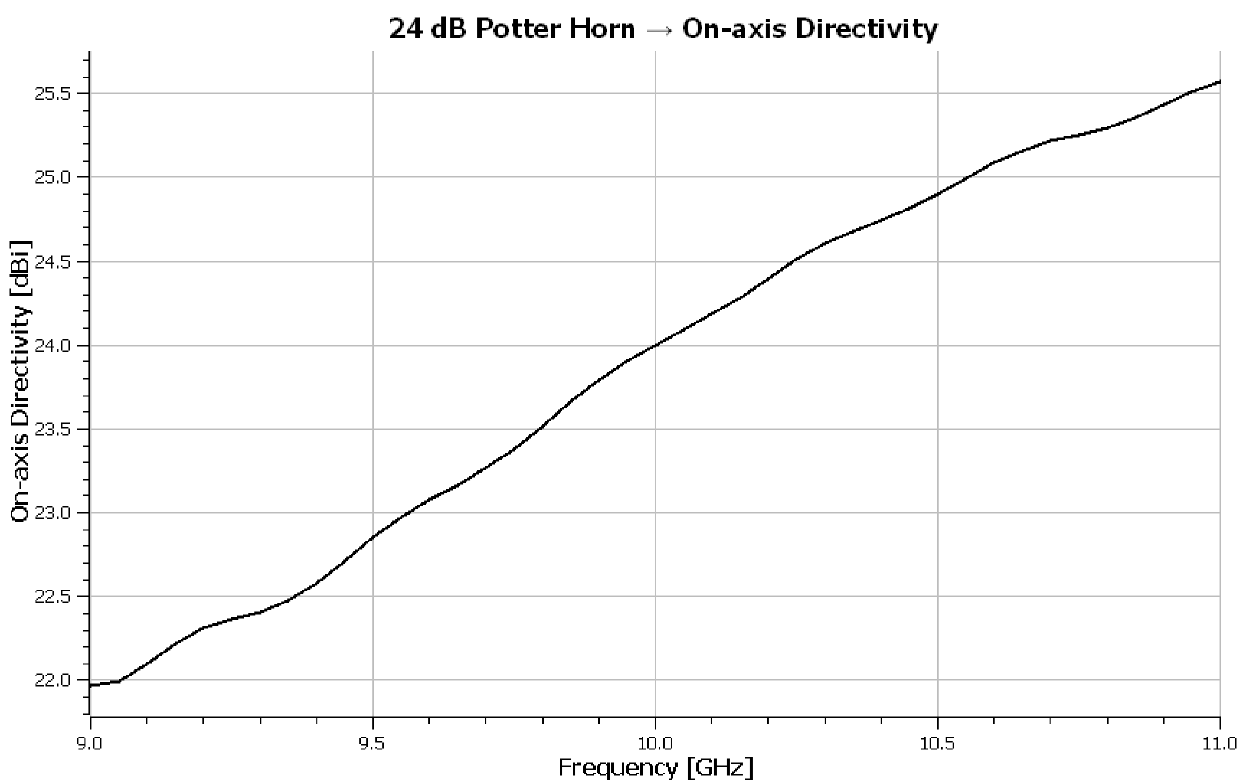

24 dB Gain Potter Horn Directivity versus Frequency

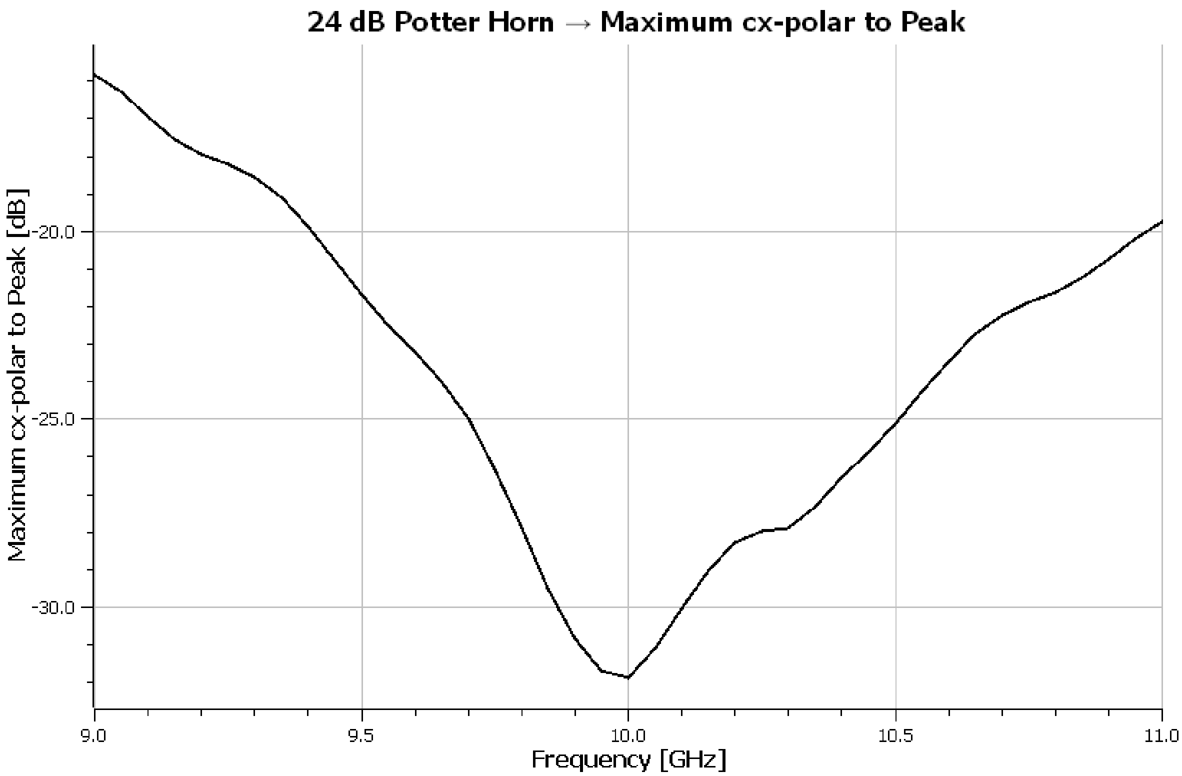

24 dB Gain Potter Horn Maximum Cross-Polarization relative to Peak versus Frequency

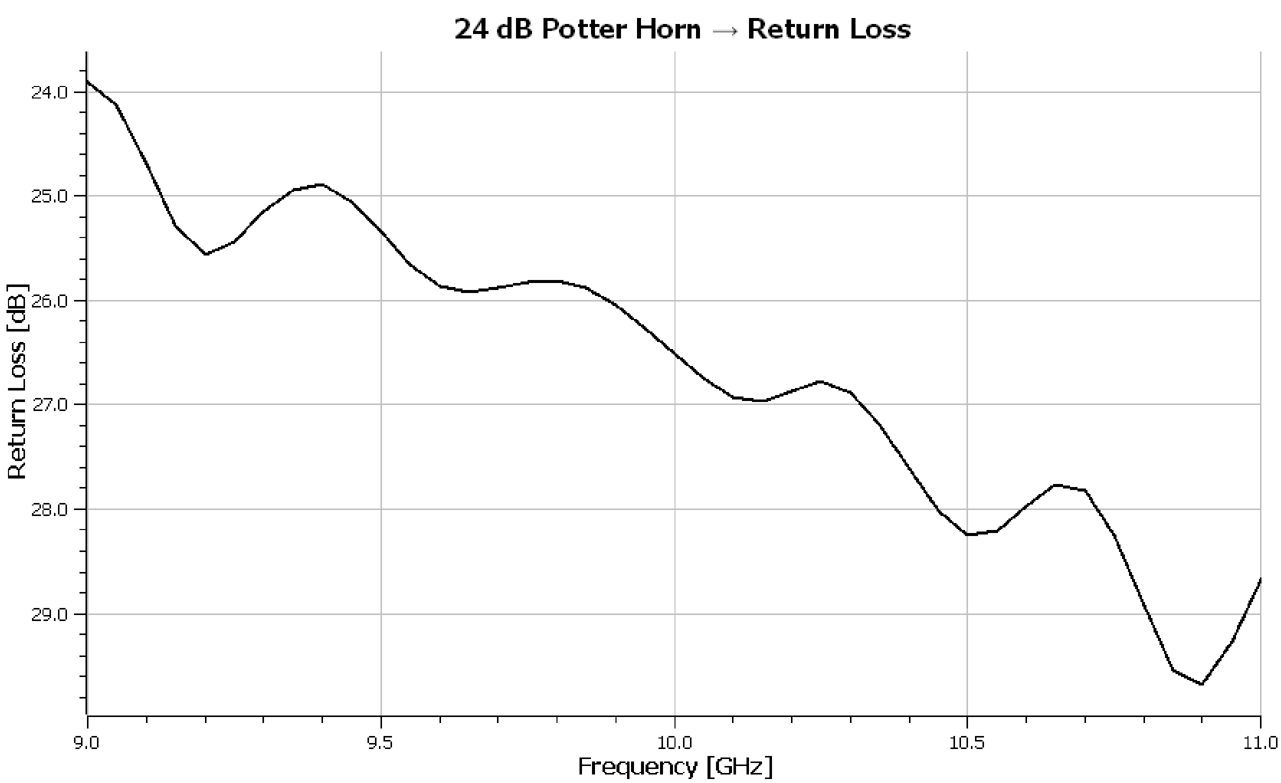

24 dB Gain Potter Horn Return Loss relative to Peak versus Frequency

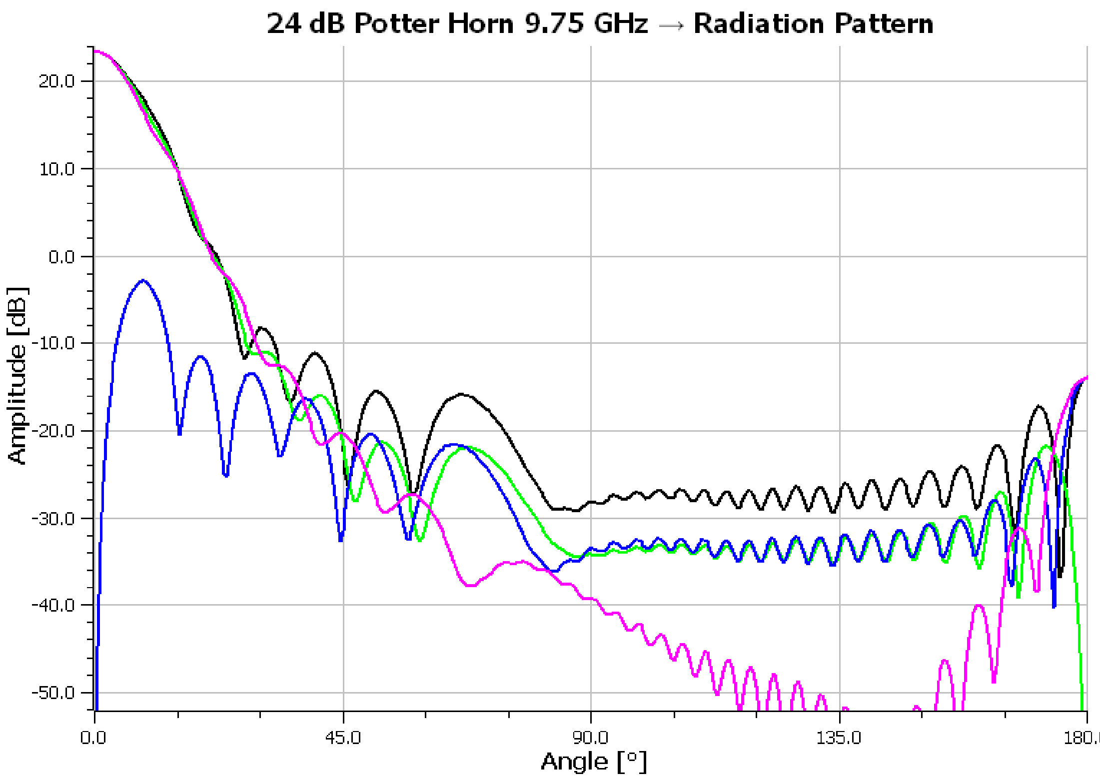

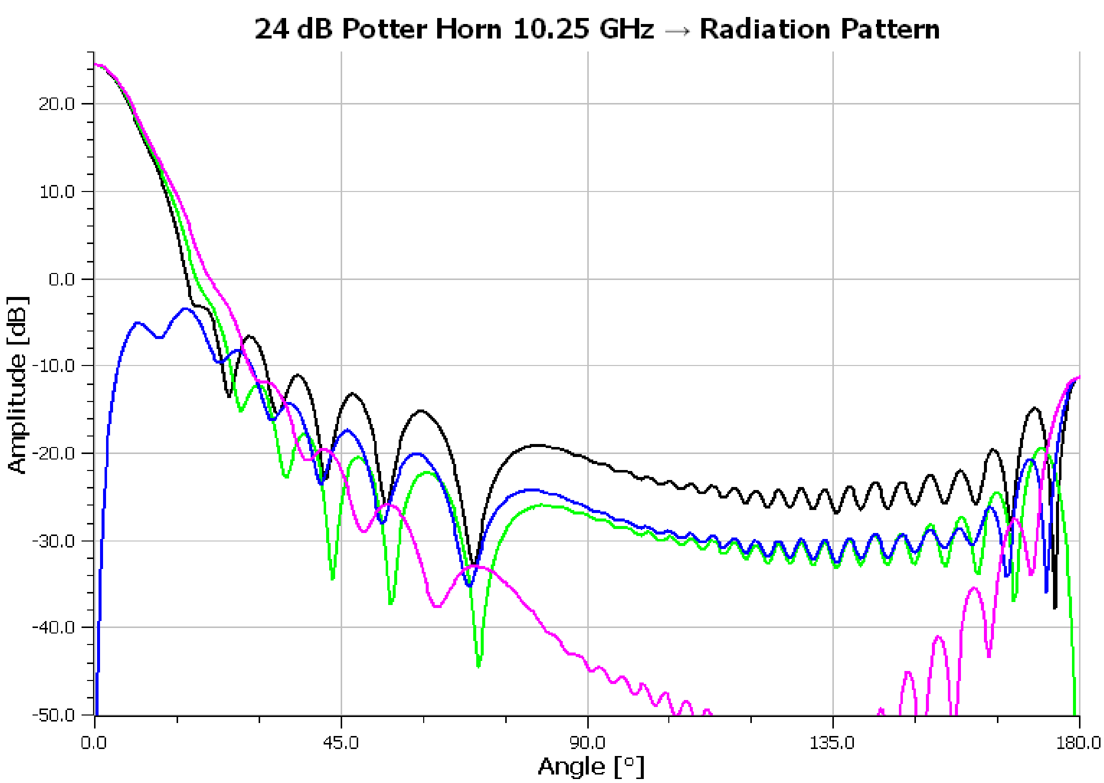

[37a] Sergei P. Skobelev, et al, "Optimum Geometry and Performance of a Dual-Mode Horn Modification," *IEEE Antennas and Propagation Magazine*, vol. 43, No. 1, February 2001, pp. 90-93.

7-9.2 Satoh Horn

The Satoh horn uses a dielectric cone inserted into a smooth-wall conical horn which generates the TM_{11} mode. The dielectric cone is placed so that corrugated performance is achieved. CHAMP (TICRA) can be used to design this horn through optimization of the parameters: gain at center frequency, maximum cross-polarization, and return loss over a small frequency range. The horn analysis uses an initial conical section from the waveguide to the dielectric cone solved by mode-matching. The rest of the horn is analyzed using BOR-MoM and includes the dielectric cone , the cone to the aperture, and the external surface of the horn. Figure 7-9.2-1 shows the location of the dielectric cone in the horn.

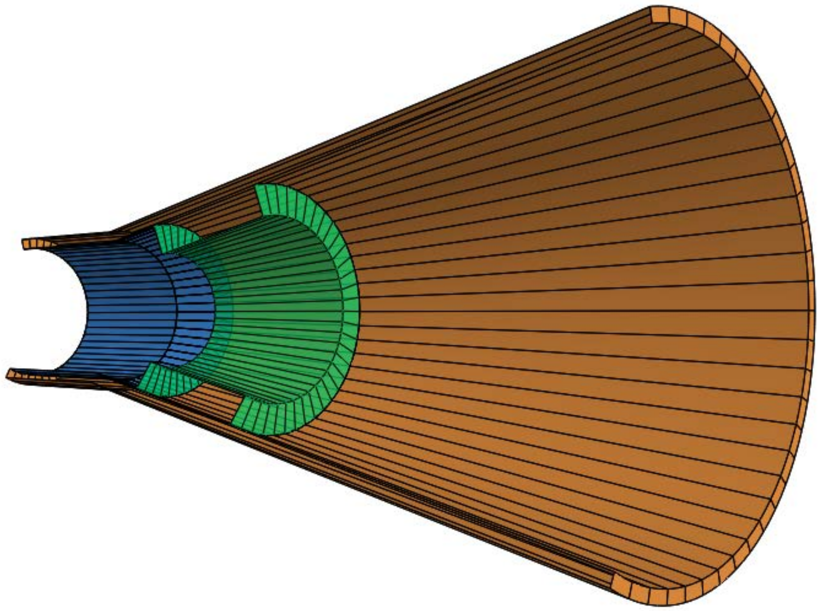

Figure 7-9.2-1 15 dB Gain Satoh Horn cross-section illustrating the dielectric cone (green) used to generate the TM_{11} mode

Table 7-9.2 lists parameters of Satoh horns designed by using the optimization of CHAMP.

Table 7-9.2 Parameters of Satoh Horns, using Teflon Cones

Gain dB	Aperture Radius, λ	Slant Length, λ	To Dielectric Step, λ	Dielectric Thickness	Cone Length, λ	25-dB X-pol BW, %	10 dB Beam-width	Phase Center, λ
15	1.0465	6.9983	0.8455	0.1640	0.9674	12.2	61.7	3.169
16	1.1550	6.2879	0.4650	0.1782	0.9439	11.4	56.1	3.269
17	1.3452	6.7636	0.4495	0.1825	0.9322	13.5	49.3	3.759
18	1.4606	8.8020	1.0936	0.1294	0.9732	19.8	43.4	4.610
19	1.6719	9.8613	1.2722	0.1344	0.9555	19.2	38.8	5.174
20	1.8134	10.335	1.0933	0.1089	1.4908	15.2	34.7	6.363
21	2.2153	11.392	1.0235	0.1364	0.9489	20.3	30.4	5.864
22	2.7976	13.028	0.9524	0.1503	0.9343	19.7	27.2	5.823
23	3.0384	15.687	1.4148	0.1432	0.9746	15.2	24.3	8.414

The Satoh horn when optimized using CHAMP has about twice the cross-polarization bandwidth compared to the Potter horn with its single metal step.

15-dB Gain Satoh Horn Response

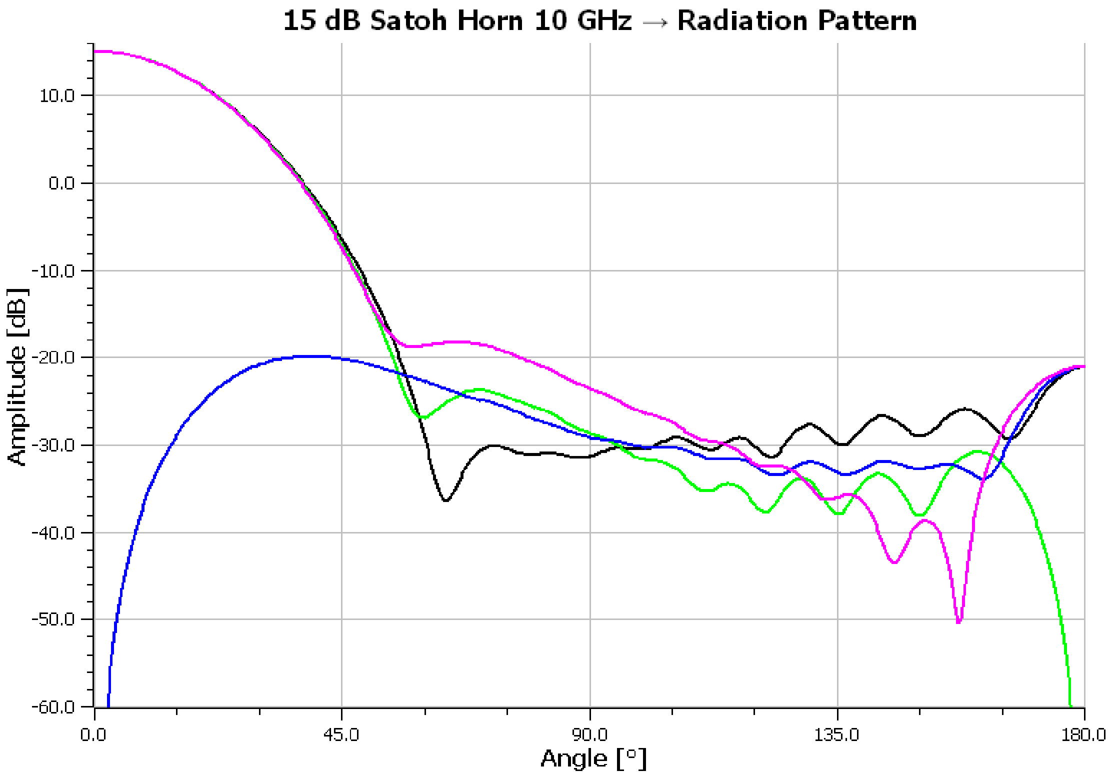

15 dB Gain Satoh Horn Center Frequency Response (10 GHz)

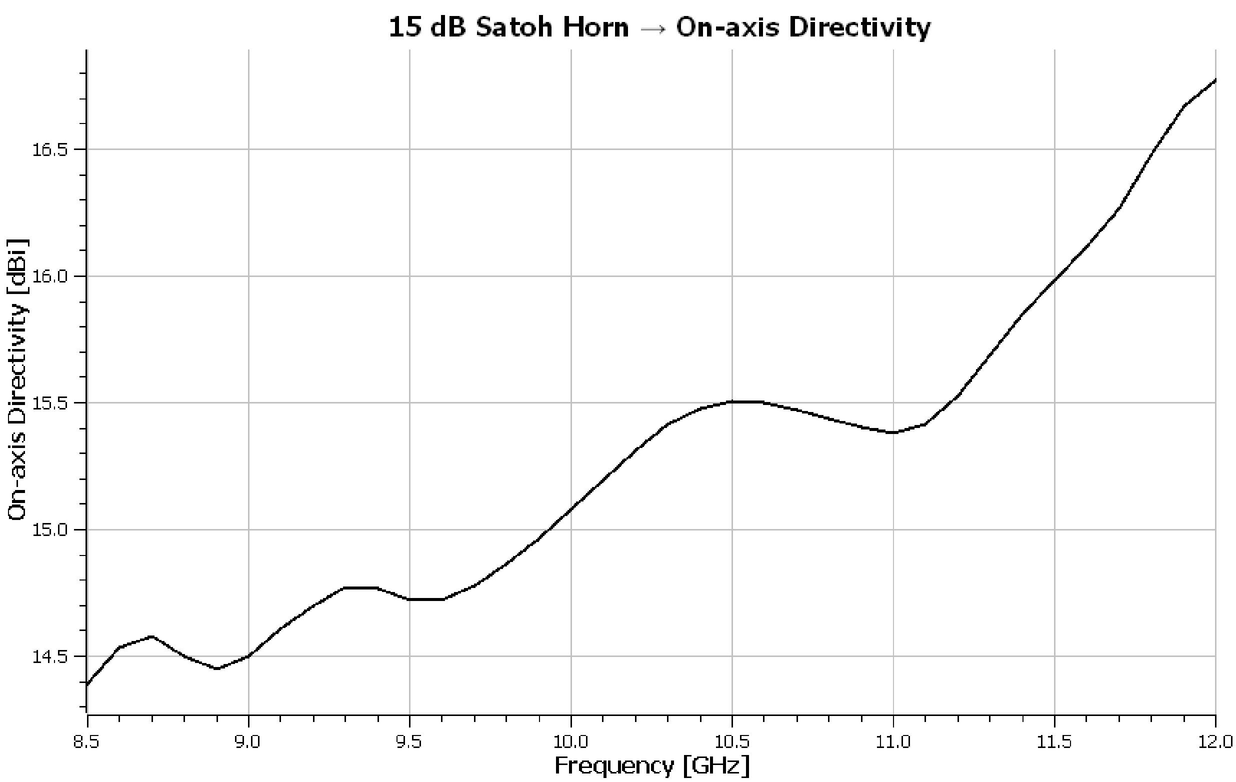

15 dB Gain Satoh Horn on axis Directivity versus Frequency

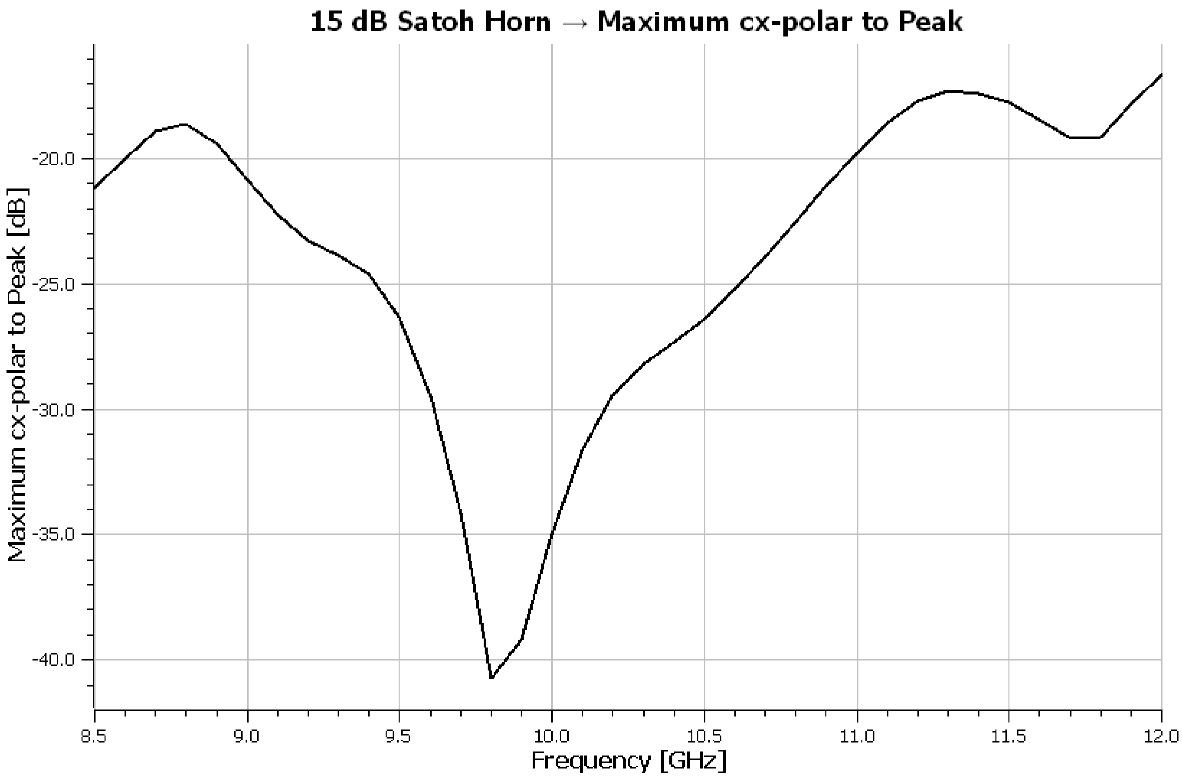

15 dB Gain Satoh Horn Maximum Cross-polarization relative to Peak Response versus Frequency

15 dB Gain Satoh Horn Return Loss versus Frequency

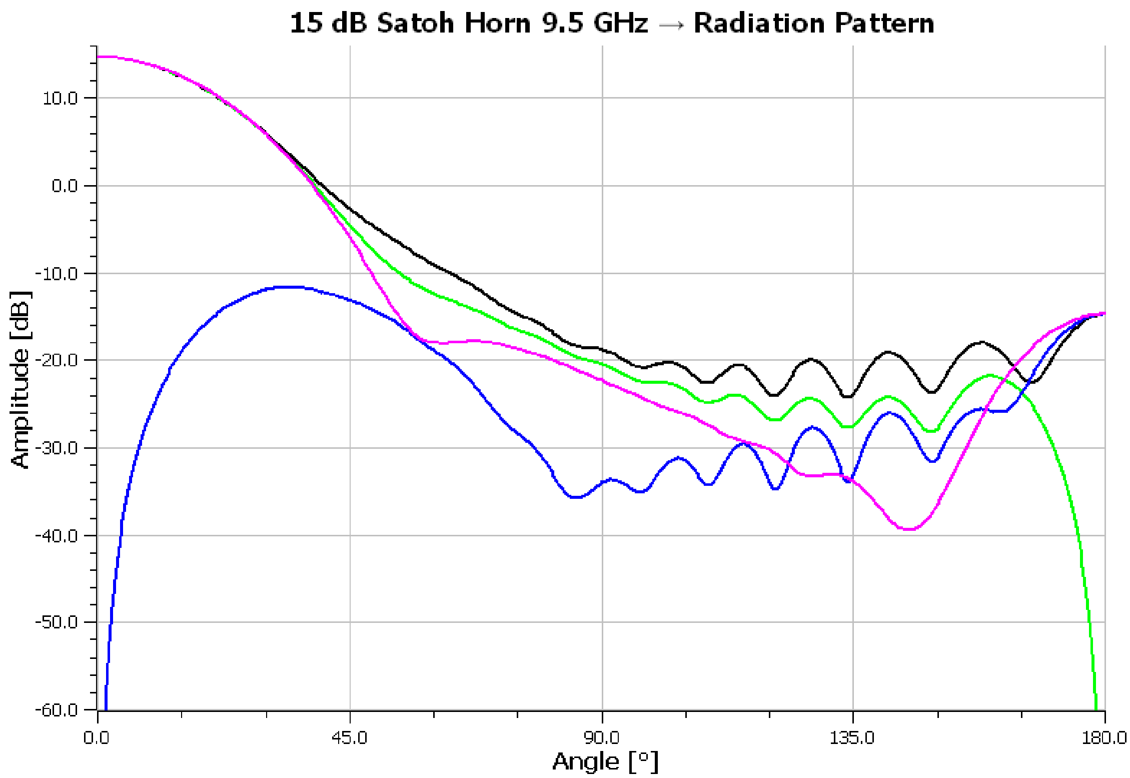
15 dB Satoh Horn 9.5 GHz → Radiation Pattern
Amplitude [dB]
10.0
0.0
-10.0
-20.0
-30.0
-40.0
-50.0
-60.0
0.0
45.0
90.0
135.0
180.0
Angle [°]

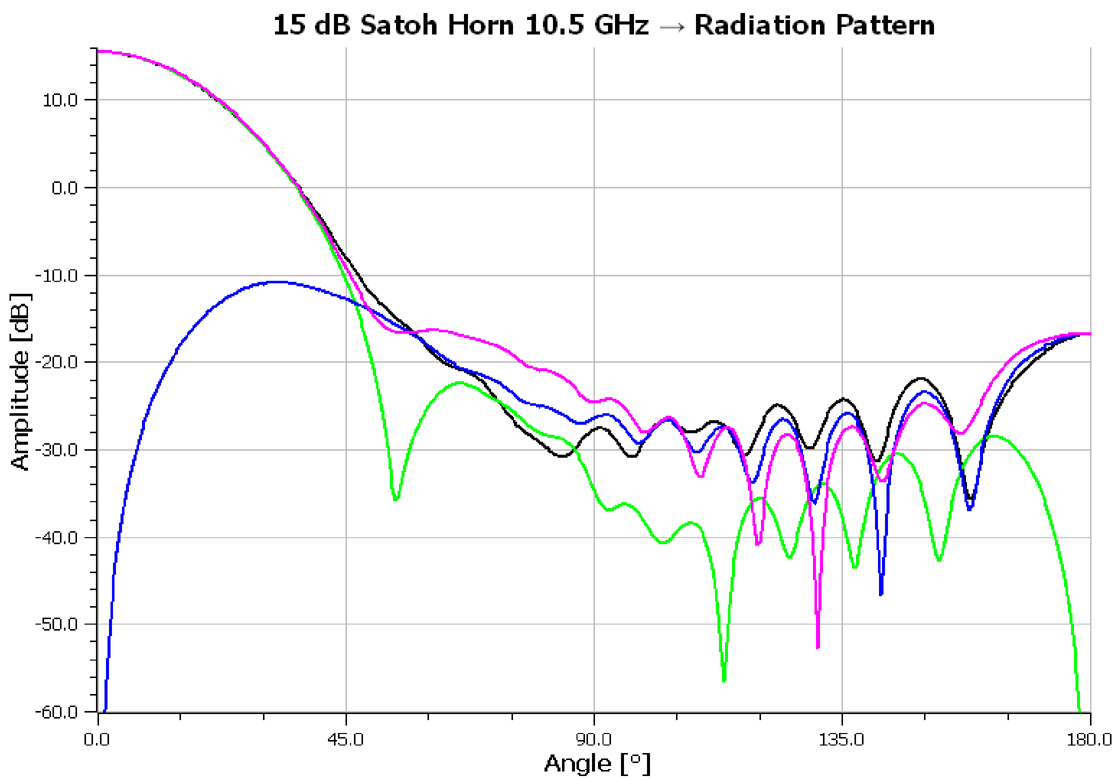
15 dB Satoh Horn 10.5 GHz → Radiation Pattern
Amplitude [dB]
10.0
0.0
-10.0
-20.0
-30.0
-40.0
-50.0
-60.0
0.0
45.0
90.0
135.0
180.0
Angle [°]

20-dB Gain Satoh Horn Design

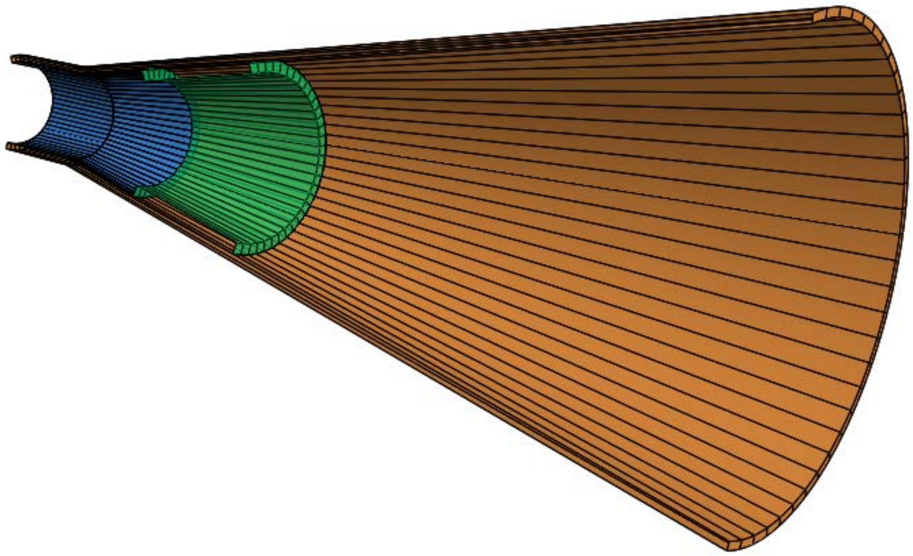

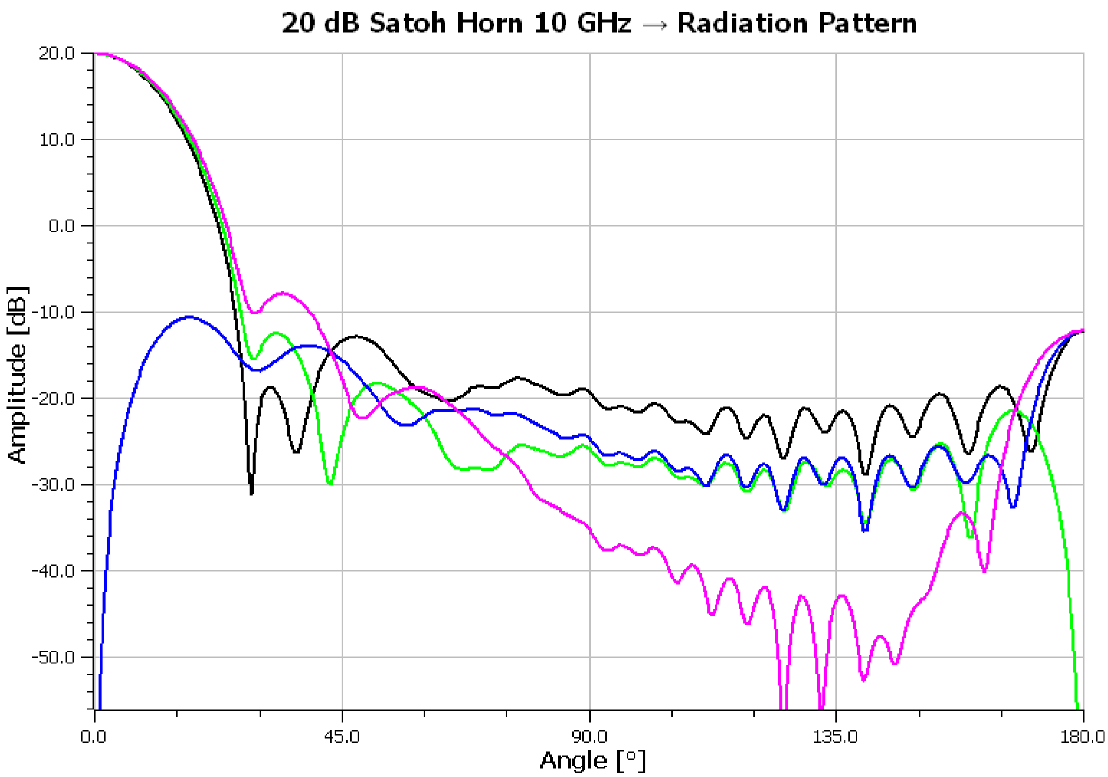

20 dB Gain Satoh Horn Center Frequency Response (10 GHz)

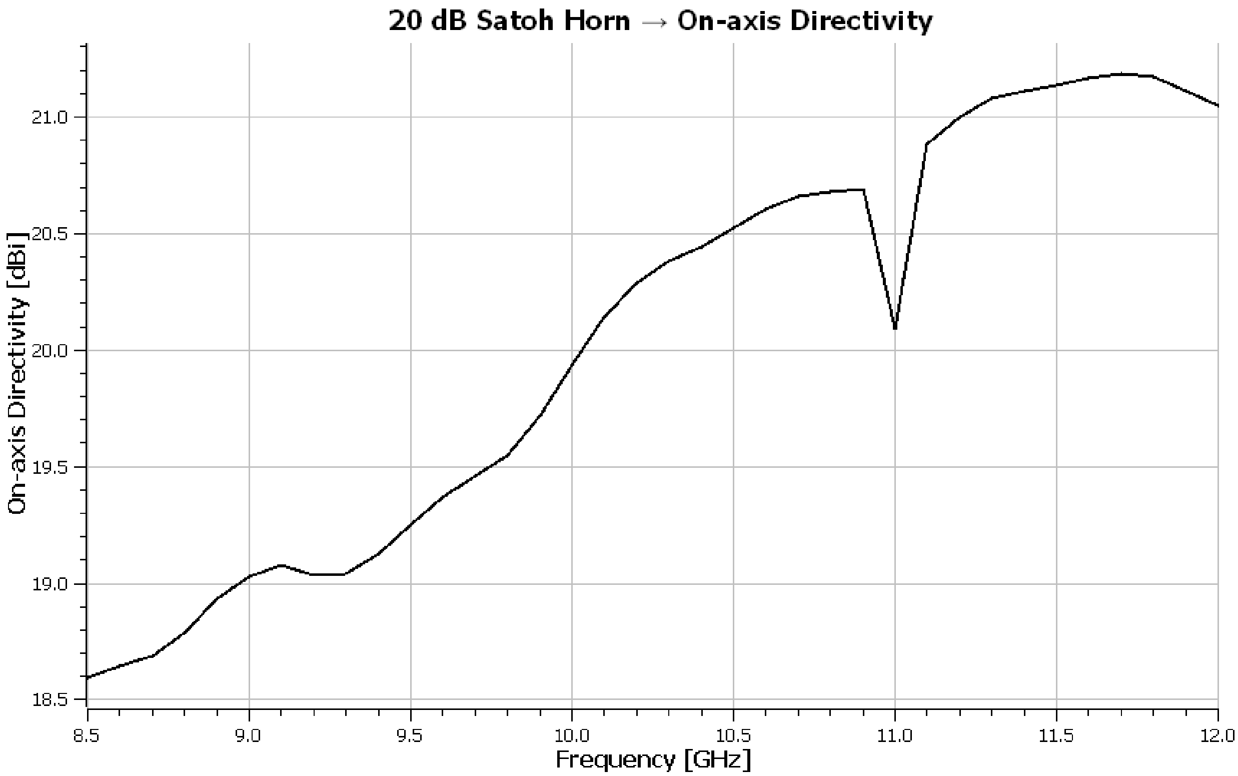

20 dB Gain Satoh Horn on axis Directivity versus Frequency

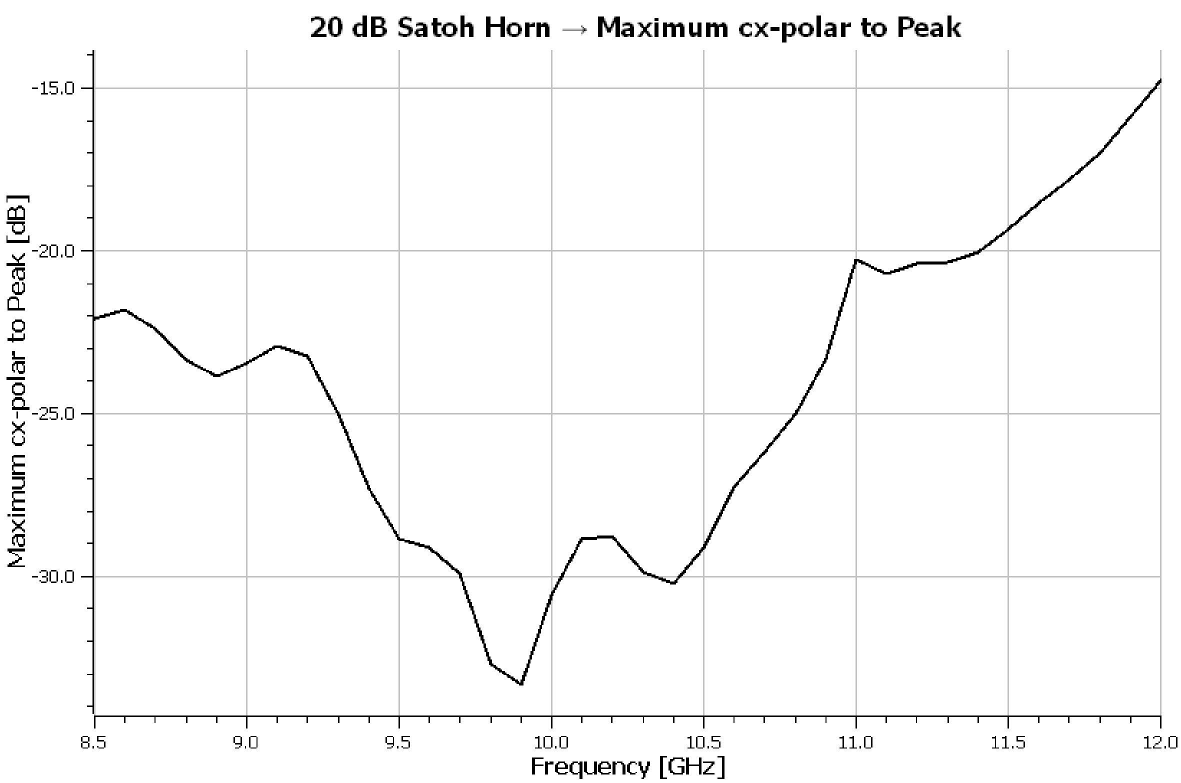

20 dB Gain Satoh Horn Maximum Cross-polarization relative to Peak Response versus Frequency

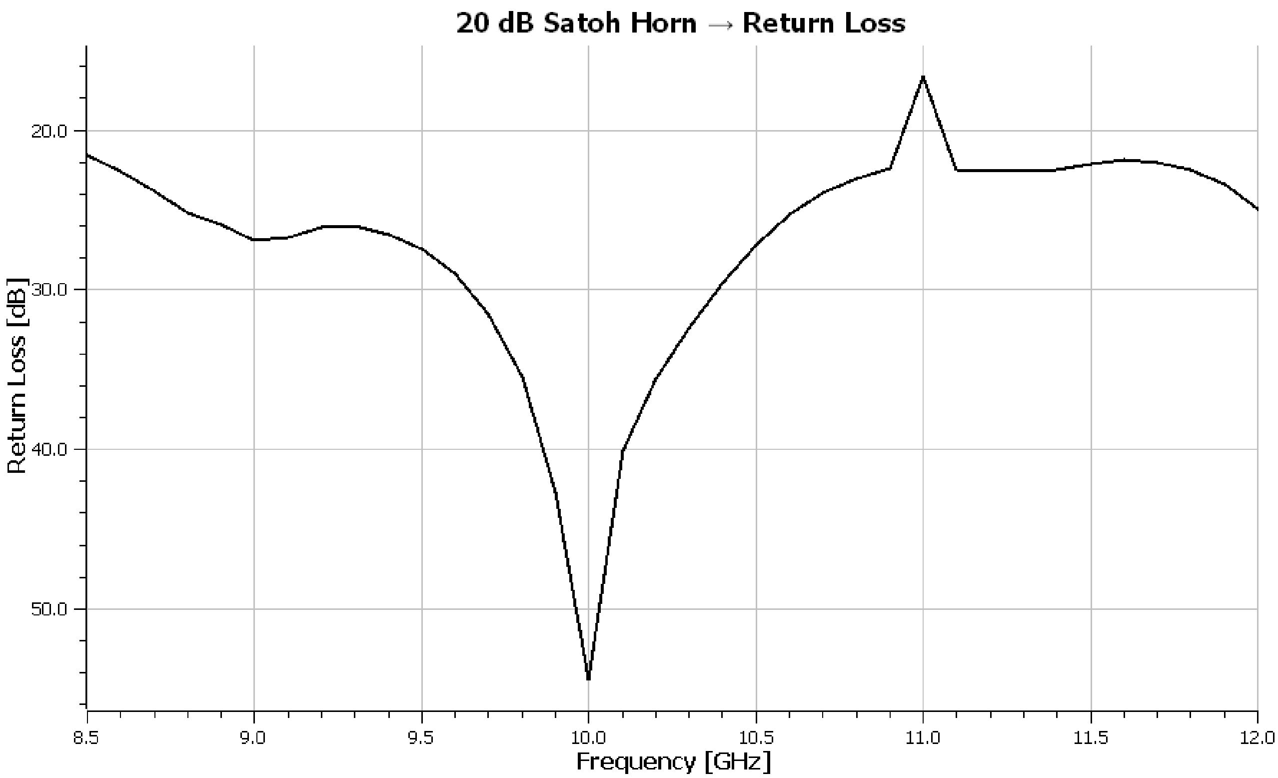

20 dB Gain Satoh Horn Return Loss versus Frequency

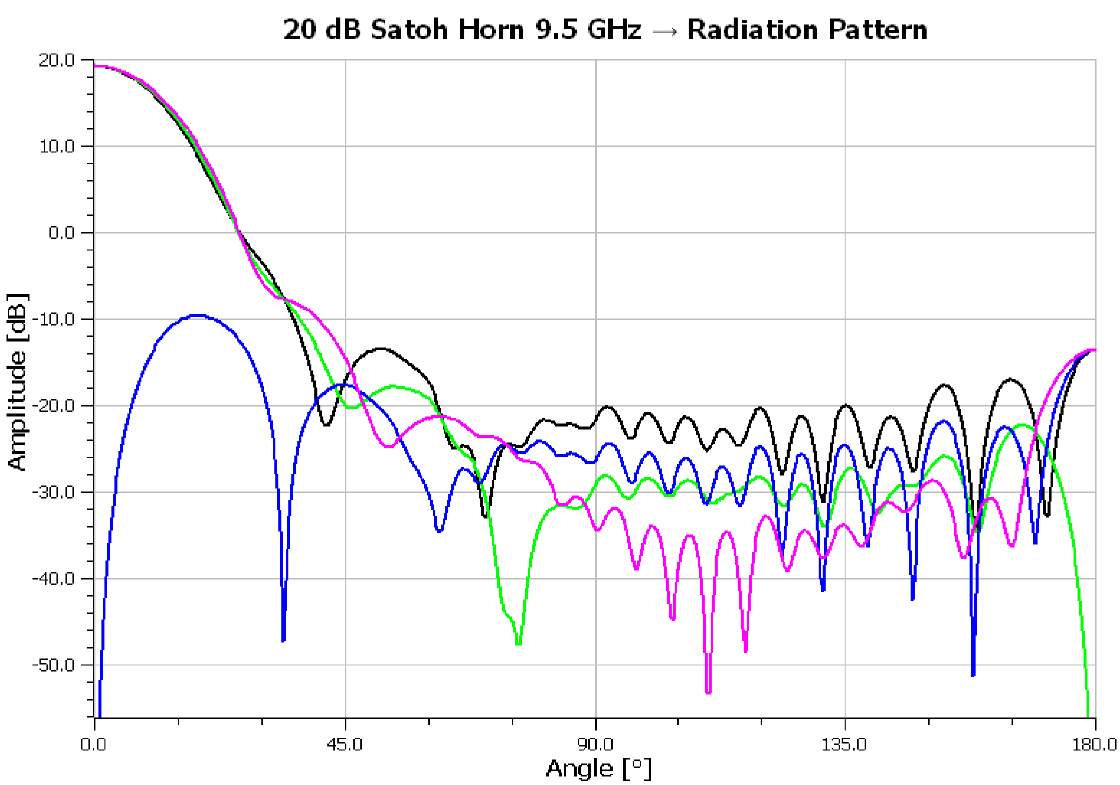

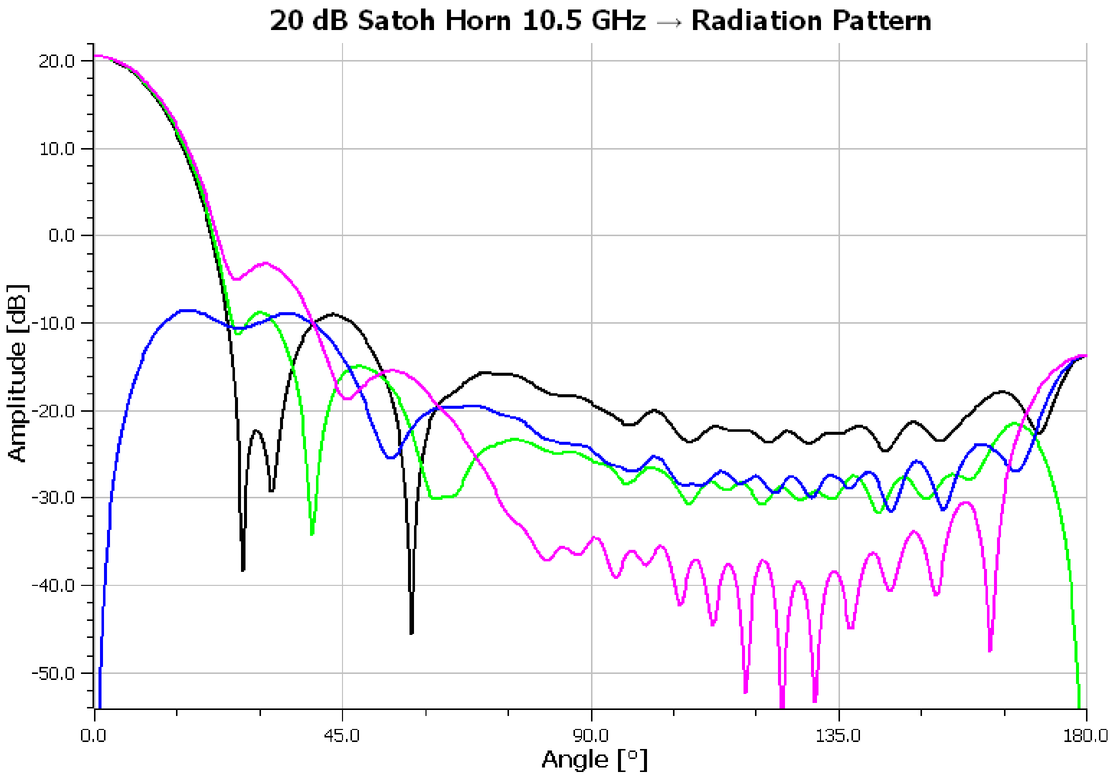
20 dB Satoh Horn 10.5 GHz → Radiation Pattern
Amplitude [dB]
20.0
10.0
0.0
-10.0
-20.0
-30.0
-40.0
-50.0
0.0
45.0
90.0
135.0
180.0
Angle [°]

23-dB Gain Satoh Horn Design

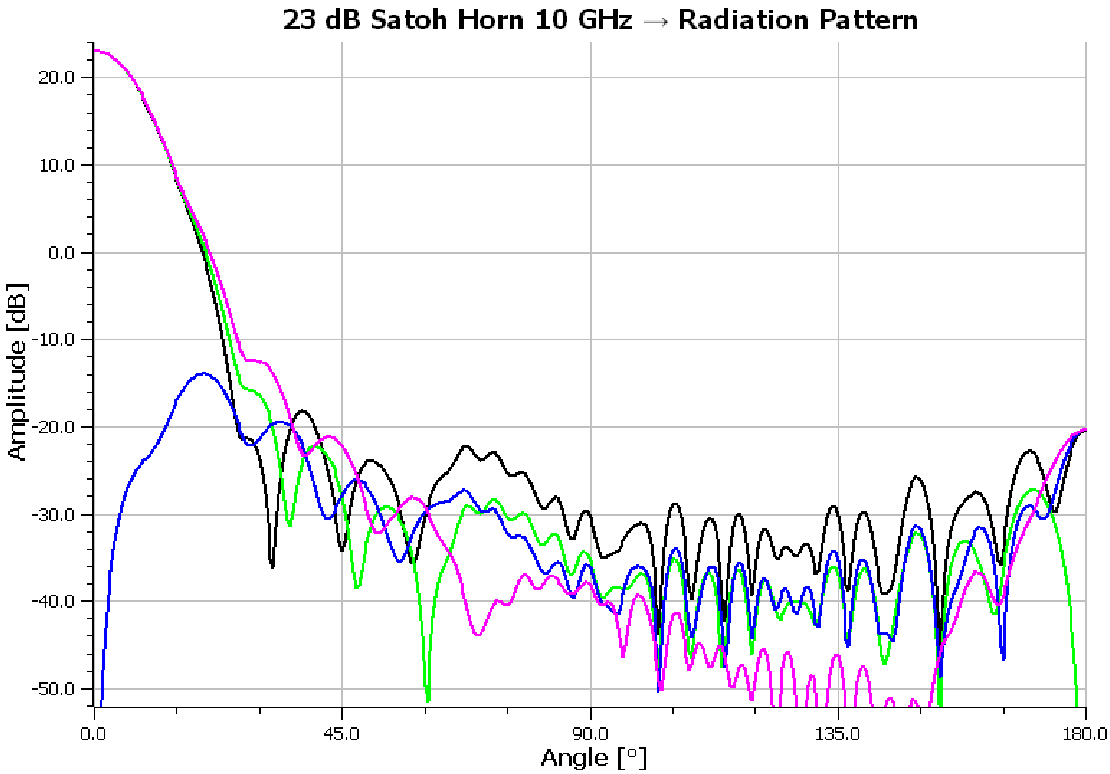

23 dB Gain Satoh Horn Center Frequency Response (10 GHz)

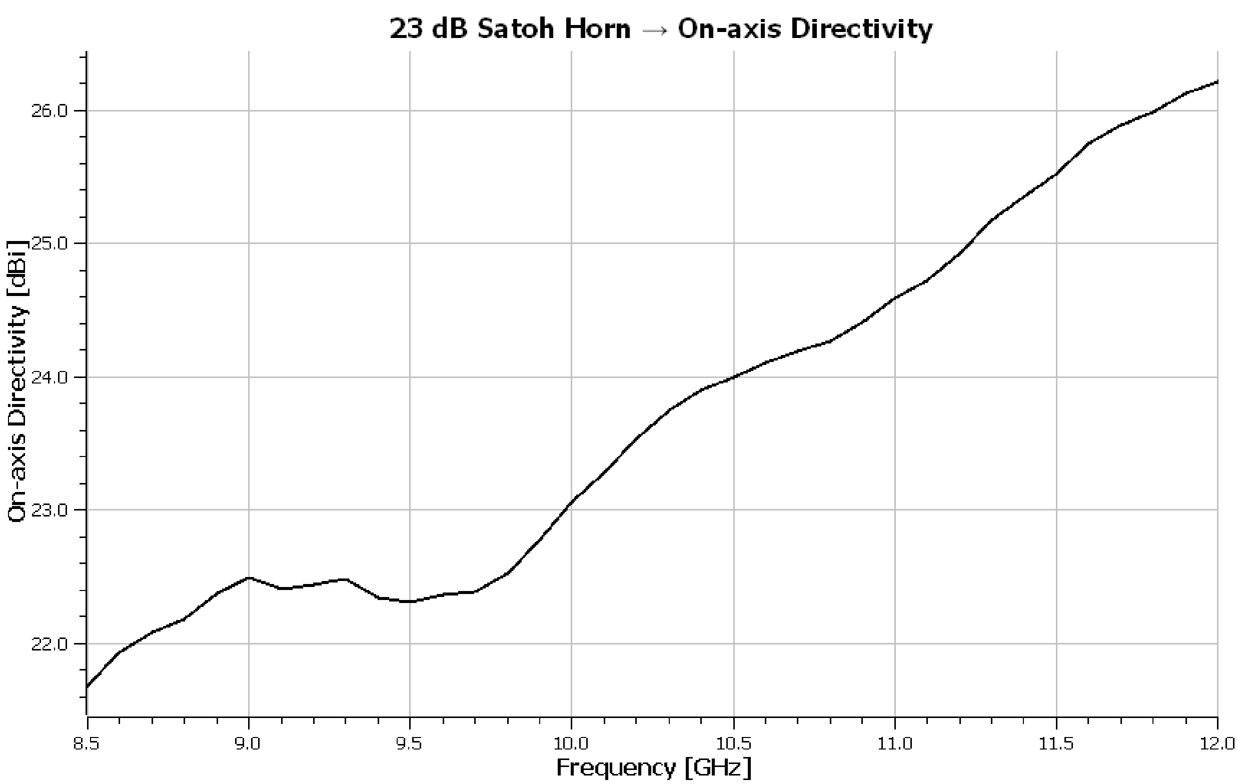

23 dB Gain Satoh Horn on axis Directivity versus Frequency

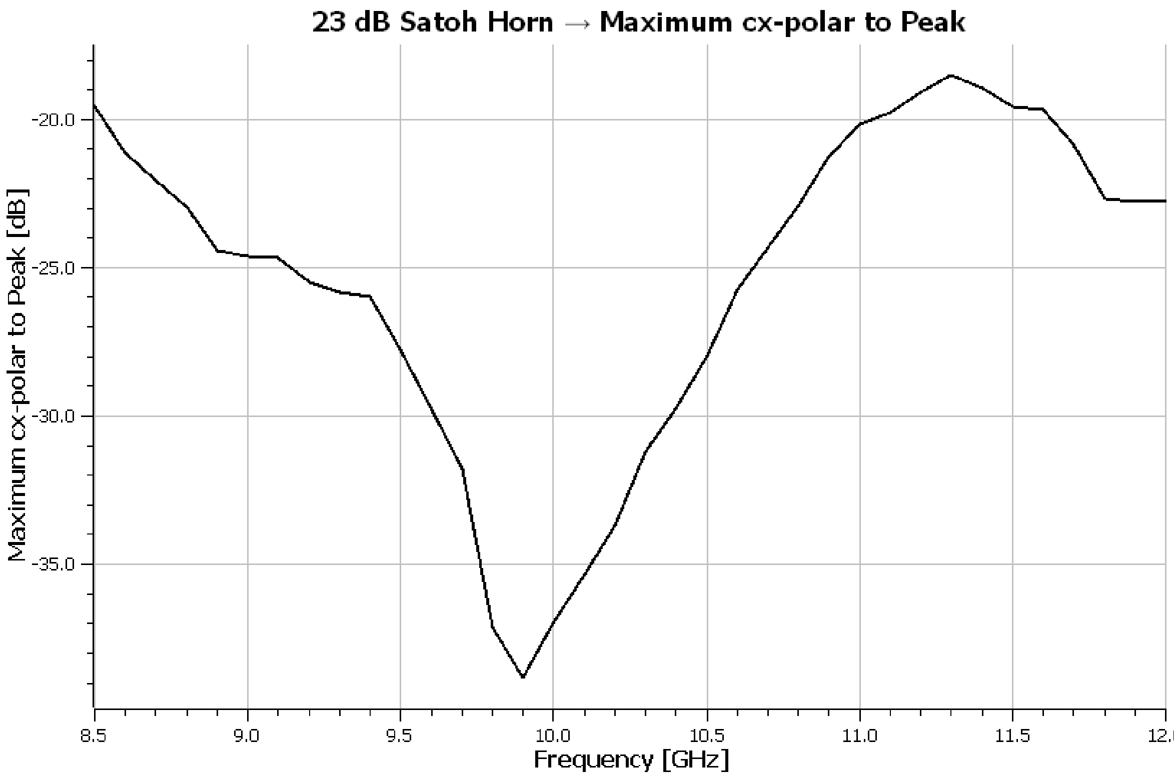

23 dB Gain Satoh Horn Maximum Cross-polarization relative to Peak Response versus Frequency

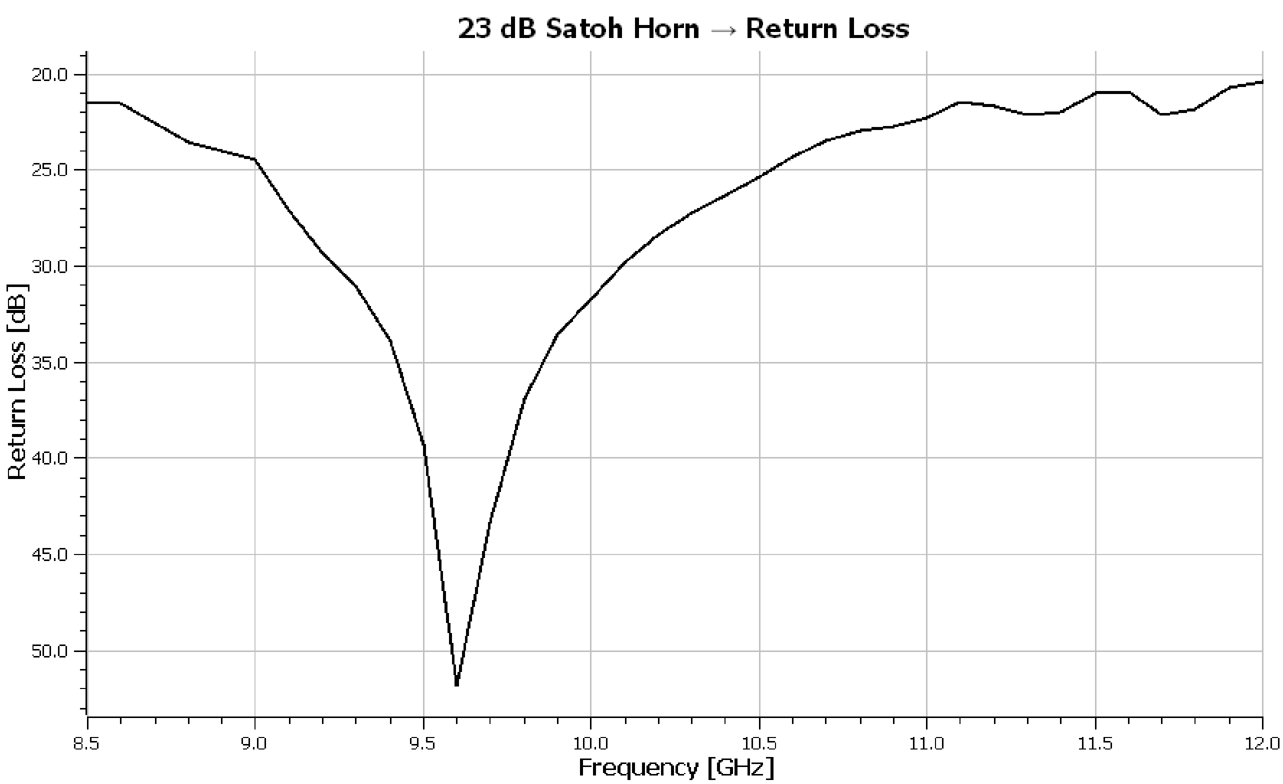

23 dB Gain Satoh Horn Return Loss versus Frequency

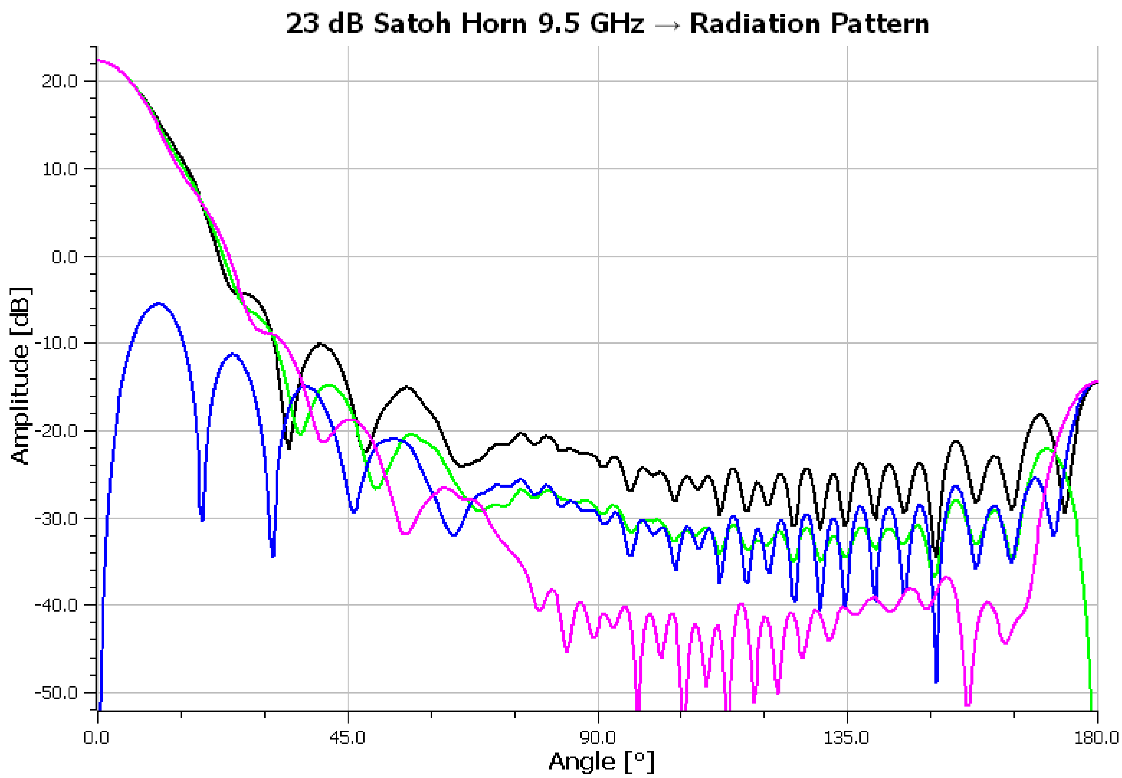
23 dB Satoh Horn 9.5 GHz → Radiation Pattern
Amplitude [dB]
Angle [°]
20.0
10.0
0.0
-10.0
-20.0
-30.0
-40.0
-50.0
0.0
45.0
90.0
135.0
180.0

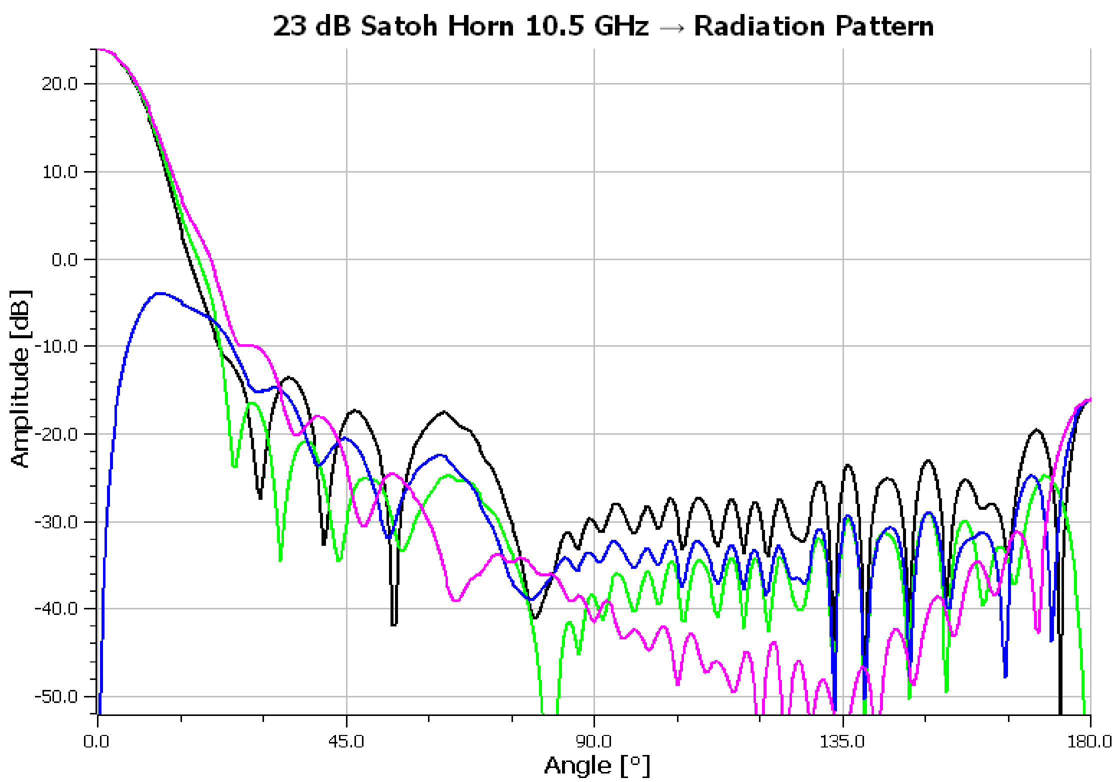
23 dB Satoh Horn 10.5 GHz → Radiation Pattern
Amplitude [dB]
Angle [°]
20.0
10.0
0.0
-10.0
-20.0
-30.0
-40.0
-50.0
0.0
45.0
90.0
135.0
180.0

7-9.3 Turrin Horn[37b]

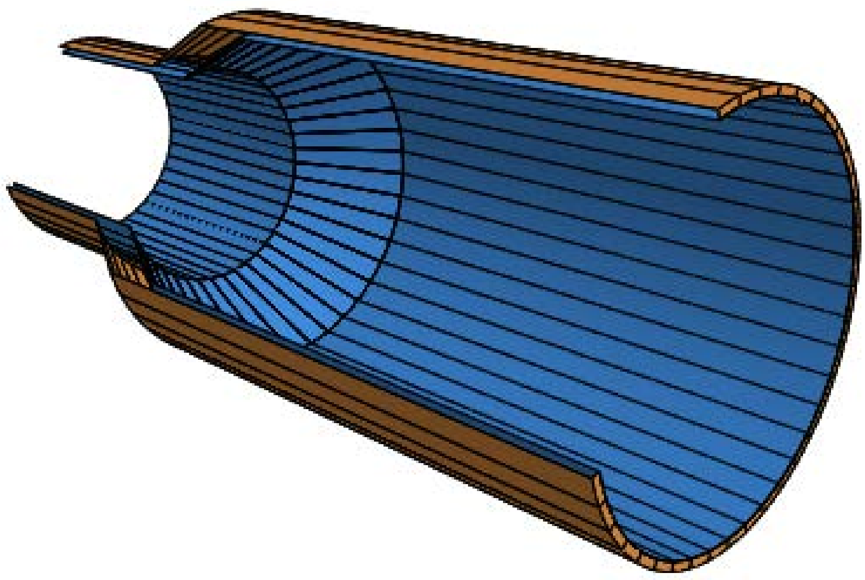

Figure 7-9.3 Turrin Horn

The Turrin horn starts with a short conical section with a cone angle of 23° to 30° and then is followed by a cylindrical section to phase the relative response of the TM_{11} generated by the transitions to generate the hybrid mode. The original article only gives a notional design procedure that relies on empirical parameter adjustment. The optimization portion within mode-matching analysis program CHAMP was used to produce the design table below. The Turrin horn radiates hybrid mode patterns over the range of 11.5- to 13.1-dB. The optimization parameters were the length of the conical and output cylindrical sections. The currents excited on the external surface of the horn must be included in the optimization because of the low gain. The bell cone angle was calculated from the output dimensions.

Table 7-9.3 Turrin Horn Designs, λ_c, a_i = 0.477 λ_c

Outer Radius, λ	Gain dB	10dB Beamwidth	Conical Length, λ	Cylindrical Length, λ	Cone Angle	Cross Polarization
0.62	11.46	95.5	0.3522	1.0787	22.0	32
0.64	11.54	94.6	0.5212	1.1637	17.7	32
0.66	11.67	93.3	0.4224	1.5411	23.4	41
0.68	11.51	95.1	0.4220	1.6939	25.7	33.1
0.70	11.99	89.7	0.4477	2.0458	26.5	39.2
0.72	12.00	89.6	0.4754	2.1293	27.1	43.2
0.74	12.31	86.4	0.5592	2.2470	25.2	36.4
0.76	12.45	84.9	0.5193	2.5886	28.6	43.7
0.78	12.62	83.2	0.5847	2.7213	27.4	50
0.80	12.80	81.4	0.6084	2.9008	28.0	42
0.82	12.94	80.1	0.5829	3.1436	30.5	50
0.84	13.12	78.3	0.6152	3.2341	30.5	40

The antenna has about a 10% 25-dB cross polarization bandwidth. The long length of the output cylinder required to phase the two modes to form the hybrid mode causes narrow bandwidth. The response shows narrow frequency regions of quickly varying parameters. The Scrimp horn has a wider bandwidth and smaller size.

0.72λ Outer Radius Turrin Horn

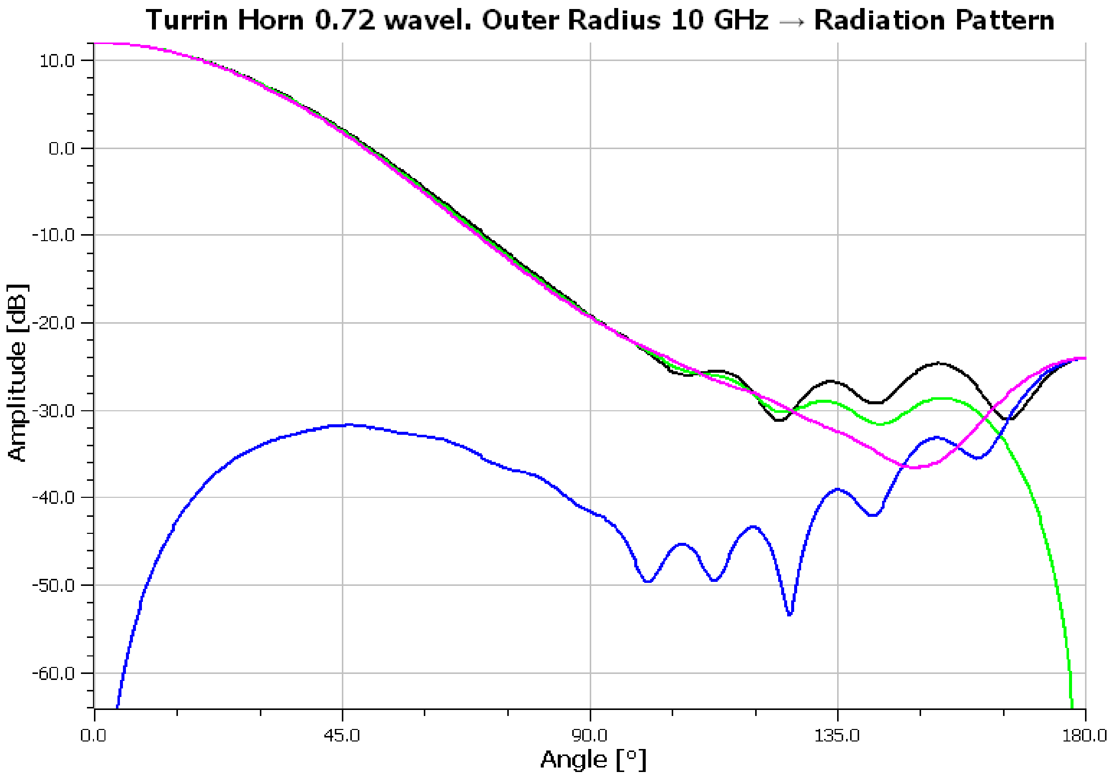

0.72λ Outer Radius Turrin Horn Center Frequency Response (10 GHz)

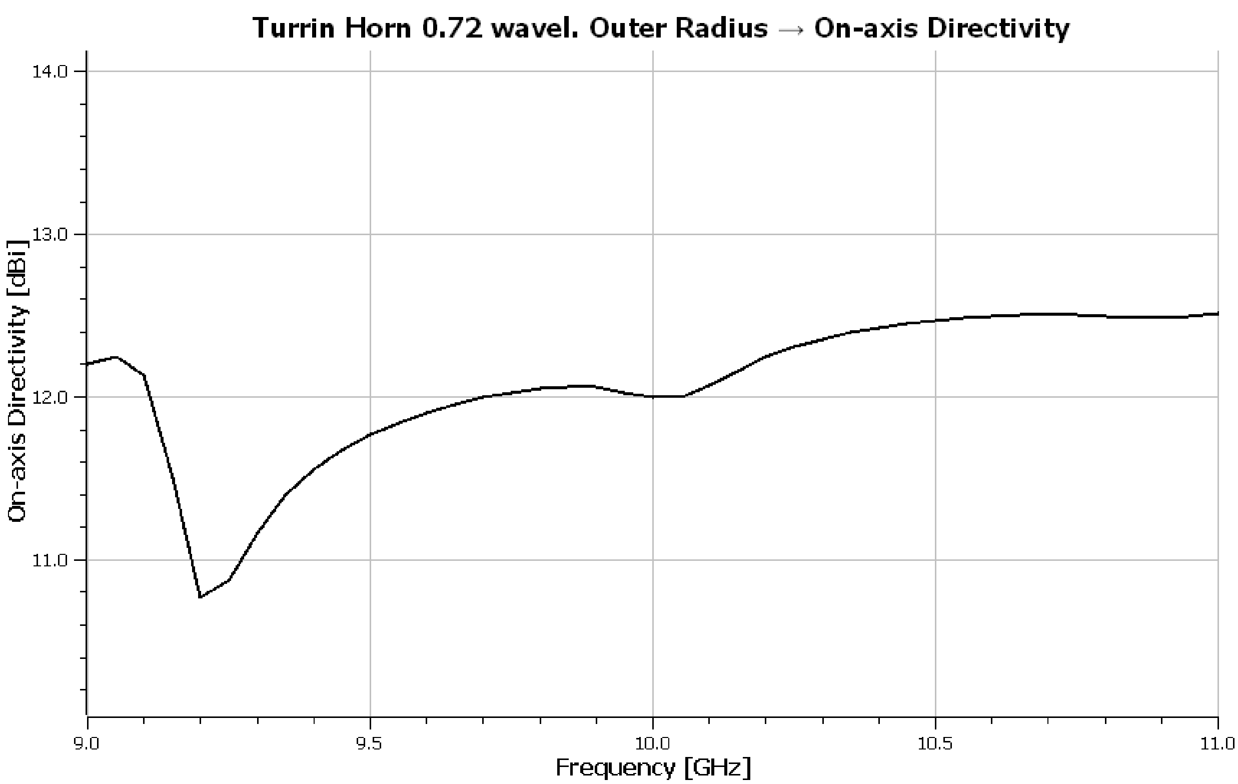

0.72λ Outer Radius Turrin Horn Gain versus Frequency

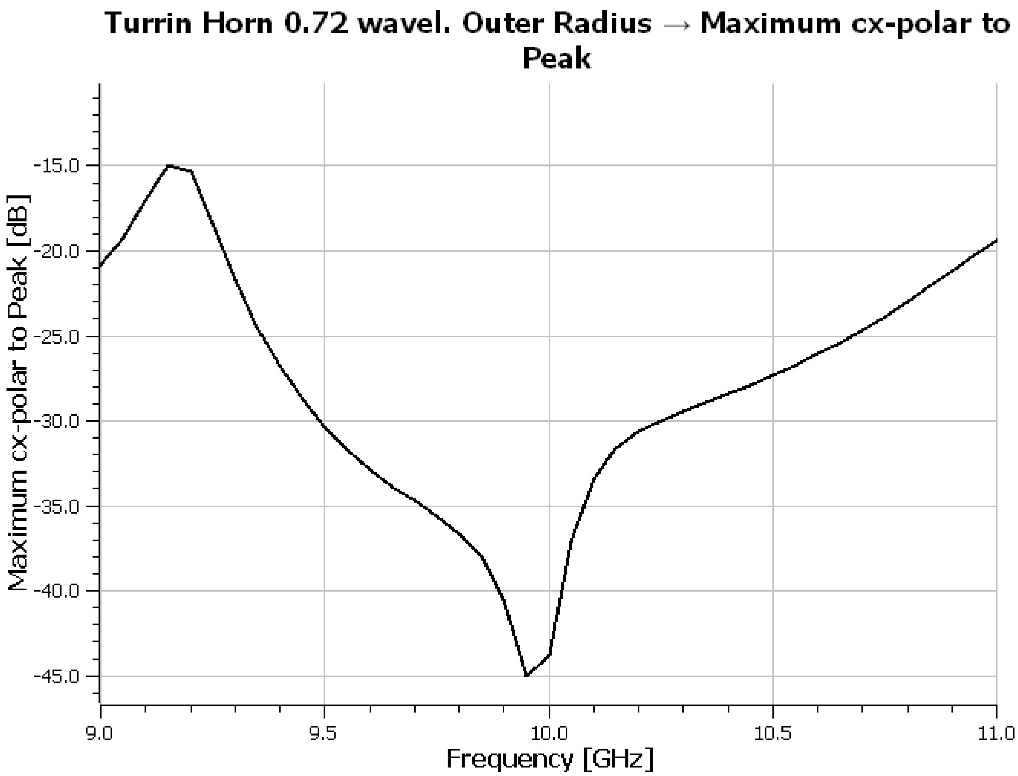

0.72λ Outer Radius Turrin Horn Maximum Cross-Polarization relative Peak versus Frequency

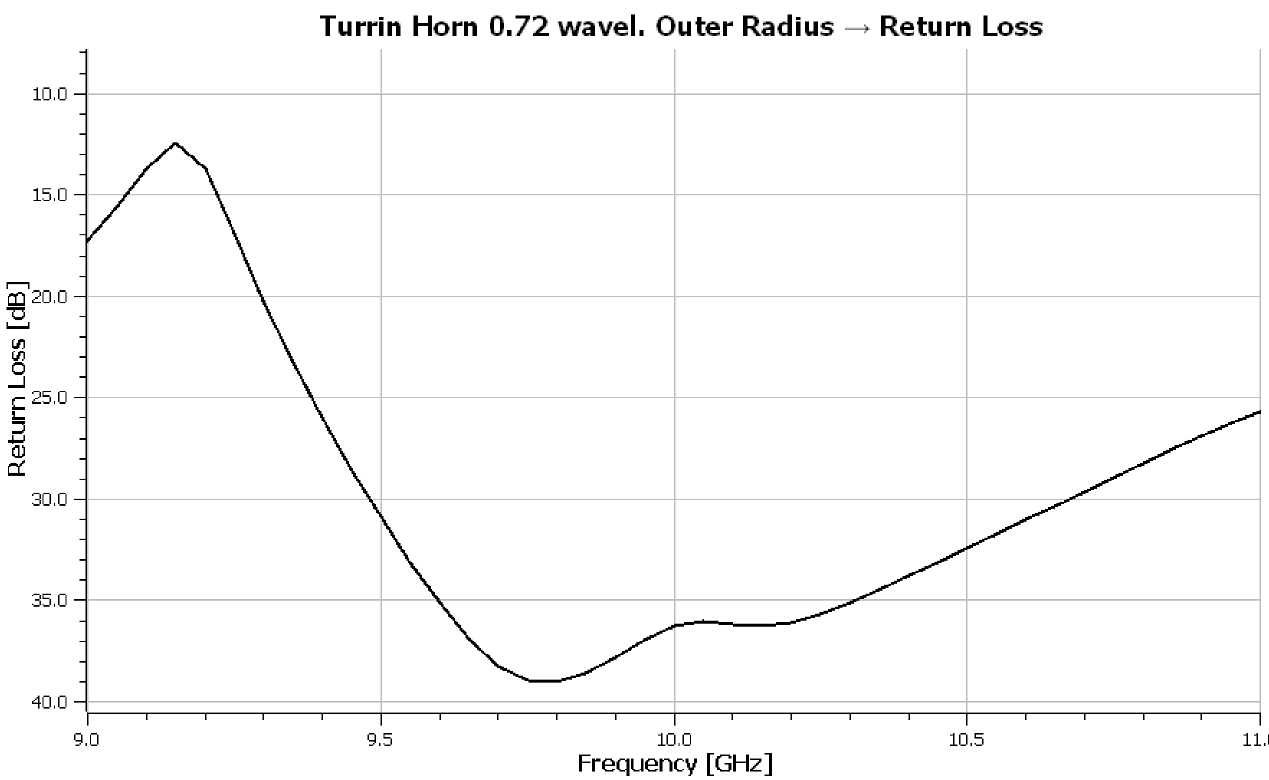

0.72λ Outer Radius Turrin Horn Return Loss versus Frequency

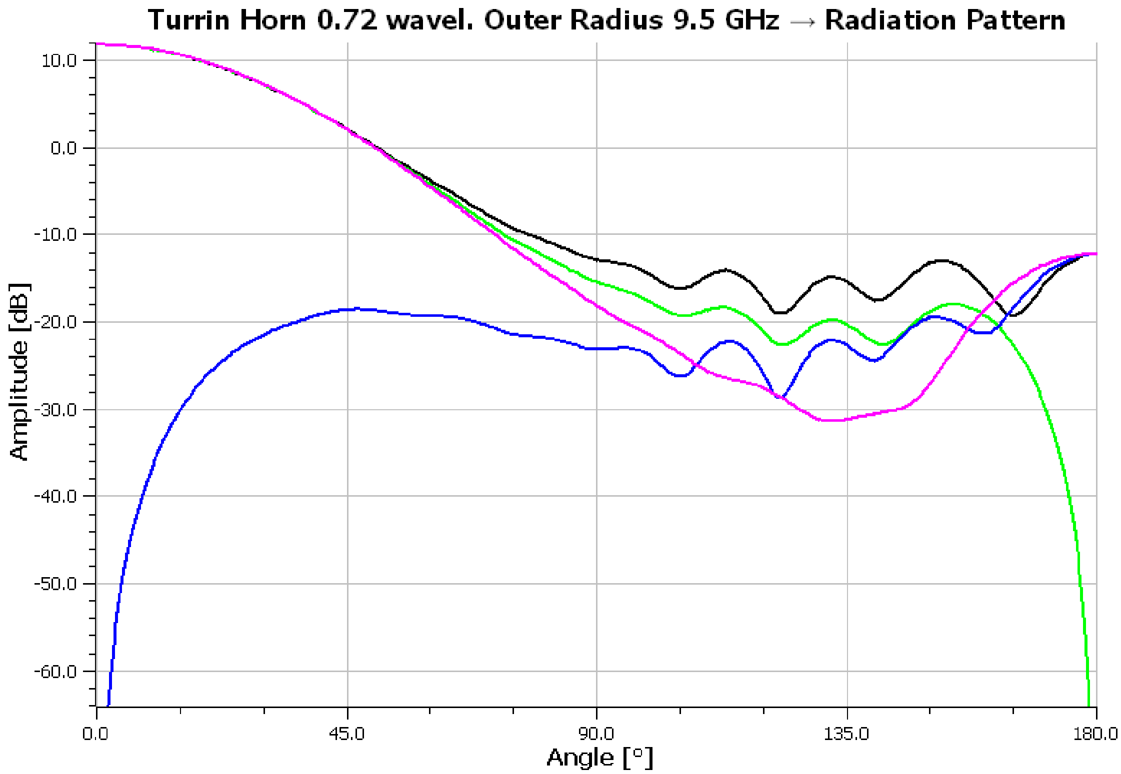

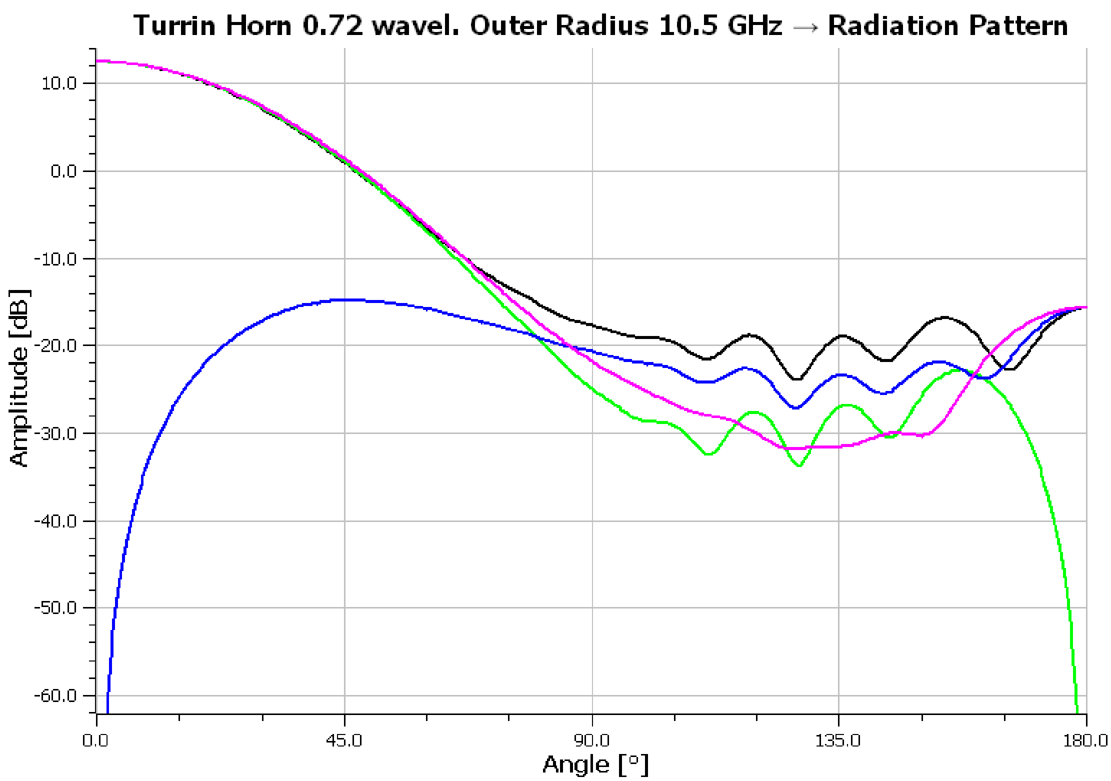

[37b] R. H. Turrin, Dual Mode Small-Aperture Antennas, *IEEE Antennas and Propagation Transactions*, Vol. xx, No. 3, March 1966, pp. 307-308.